

# 从 mono- $Z$ 信号中搜寻暗物质

余钊焕

February 24, 2014

## 目录

1	暗物质有效算符	2
2	轻子道	4
3	强子道	9
4	实验灵敏度	14
5	极化束流	14
A	模型检验	19
A.1	算符 $\mathcal{O}_{F1}$	19
A.2	算符 $\mathcal{O}_{F2}$	21
A.3	算符 $\mathcal{O}_{FH}$	23
A.4	算符 $\mathcal{O}_{FP}$	24
A.5	算符 $\mathcal{O}_{FA}$	25
B	算符 $\mathcal{O}_{F1}$ 和 $\mathcal{O}_{F2}$ 参数对产生截面的影响	26
C	背景和信号的极化截面	27
D	末态角分布与螺旋度的关系：一个例子	27
E	赝快度 $\eta$ 与 $\theta$ 角的对应关系	28

在 LHC 上通过 mono-Z 信号搜寻暗物质参见文献 [1, 2], 这里讨论未来高能  $e^+e^-$  对撞机对此信号的探测能力.

## 1 暗物质有效算符

在  $e^+e^-$  对撞机上通过 mono-Z 信号 ( $Z + \cancel{E}$ ) 搜寻暗物质, 探测的是  $e^+e^- \rightarrow \chi\bar{\chi}Z$  过程, 可以分为两种情况: 1) 暗物质与  $Z$  玻色子耦合,  $Z$  玻色子与暗物质粒子联合产生; 2) 暗物质与电子耦合,  $Z$  玻色子来自电子的初态辐射. 如 Fig. 1 所示.

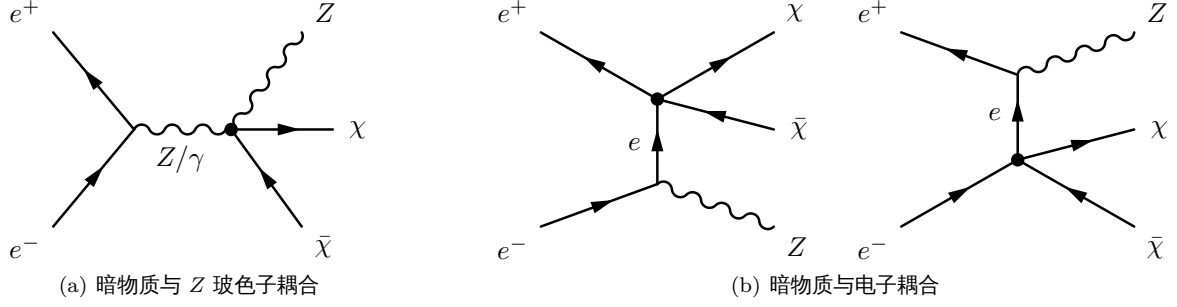


Figure 1:  $e^+e^-$  对撞机上的暗物质 mono-Z 信号.

下面假设暗物质粒子为 Dirac 费米子, 它与标准模型粒子通过有效算符耦合. 要求这些有效算符满足如下条件: (1) 暗物质粒子在标准模型规范相互作用下为单态; (2)  $SU(2)_L \times U(1)_Y$  规范不变性; (3) 存在额外的  $Z_2$  对称性使暗物质粒子稳定; (4)  $CP$  守恒.

对于暗物质粒子 ( $\chi$ ) 与  $Z$  玻色子的耦合, 我们考虑有效算符

$$\mathcal{O}_{F1} = \frac{k_1}{\Lambda_1^3} \bar{\chi} \chi B_{\mu\nu} B^{\mu\nu} + \frac{k_2}{\Lambda_2^3} \bar{\chi} \chi W_{\mu\nu}^a W^{a\mu\nu}, \quad \mathcal{O}_{F2} = \frac{k_1}{\Lambda_1^3} \bar{\chi} i \gamma_5 \chi B_{\mu\nu} \tilde{B}^{\mu\nu} + \frac{k_2}{\Lambda_2^3} \bar{\chi} i \gamma_5 \chi W_{\mu\nu}^a \tilde{W}^{a\mu\nu}, \quad (1)$$

其中  $B^{\mu\nu} \equiv \partial^\mu B^\nu - \partial^\nu B^\mu$ ,  $W^{a\mu\nu} \equiv \partial^\mu W^{a\nu} - \partial^\nu W^{a\mu} + g_2 \varepsilon^{abc} W^{b\mu} W^{c\nu}$ . 用 Weinberg 转动角  $\theta_W$  将规范场规范态表示成物理态, 有

$$B_\mu = c_W A_\mu - s_W Z_\mu, \quad W_\mu^3 = s_W A_\mu + c_W Z_\mu, \quad (2)$$

其中  $c_W \equiv \cos \theta_W = \frac{g_2}{\sqrt{g_1^2 + g_2^2}}$ ,  $s_W \equiv \sin \theta_W = \frac{g_1}{\sqrt{g_1^2 + g_2^2}}$ . 从而,

$$B_{\mu\nu} = \partial_\mu B_\nu - \partial_\nu B_\mu = c_W A_{\mu\nu} - s_W Z_{\mu\nu}, \quad (3)$$

$$\begin{aligned} W_{\mu\nu}^3 &= \partial_\mu W_\nu^3 - \partial_\nu W_\mu^3 - g_2 \varepsilon^{3bc} W_\mu^b W_\nu^c = \partial_\mu W_\nu^3 - \partial_\nu W_\mu^3 - g_2 W_\mu^1 W_\nu^2 + g_2 W_\mu^2 W_\nu^1 \\ &= s_W A_{\mu\nu} + c_W Z_{\mu\nu} - g_2 W_\mu^1 W_\nu^2 + g_2 W_\mu^2 W_\nu^1. \end{aligned} \quad (4)$$

其中  $A_{\mu\nu} \equiv \partial_\mu A_\nu - \partial_\nu A_\mu$ ,  $Z_{\mu\nu} \equiv \partial_\mu Z_\nu - \partial_\nu Z_\mu$ . 于是,

$$B_{\mu\nu} B^{\mu\nu} = c_W^2 A_{\mu\nu} A^{\mu\nu} - 2s_W c_W A_{\mu\nu} Z^{\mu\nu} + s_W^2 Z_{\mu\nu} Z^{\mu\nu}, \quad (5)$$

$$W_{\mu\nu}^3 W^{3\mu\nu} = s_W^2 A_{\mu\nu} A^{\mu\nu} + 2s_W c_W A_{\mu\nu} Z^{\mu\nu} + c_W^2 Z_{\mu\nu} Z^{\mu\nu} + \dots. \quad (6)$$

故

$$\frac{k_1}{\Lambda_1^3} B_{\mu\nu} B^{\mu\nu} + \frac{k_2}{\Lambda_2^3} W_{\mu\nu}^3 W^{3\mu\nu} = G_{AA} A_{\mu\nu} A^{\mu\nu} + G_{AZ} A_{\mu\nu} Z^{\mu\nu} + G_{ZZ} Z_{\mu\nu} Z^{\mu\nu} + \dots, \quad (7)$$

$$\frac{k_1}{\Lambda_1^3} B_{\mu\nu} \tilde{B}^{\mu\nu} + \frac{k_2}{\Lambda_2^3} W_{\mu\nu}^3 \tilde{W}^{3\mu\nu} = G_{AA} A_{\mu\nu} \tilde{A}^{\mu\nu} + G_{AZ} A_{\mu\nu} \tilde{Z}^{\mu\nu} + G_{ZZ} Z_{\mu\nu} \tilde{Z}^{\mu\nu} + \dots, \quad (8)$$

其中

$$G_{AA} \equiv \frac{k_1 c_W^2}{\Lambda_1^3} + \frac{k_2 s_W^2}{\Lambda_2^3}, \quad G_{AZ} \equiv 2s_W c_W \left( \frac{k_2}{\Lambda_2^3} - \frac{k_1}{\Lambda_1^3} \right), \quad G_{ZZ} \equiv \frac{k_1 s_W^2}{\Lambda_1^3} + \frac{k_2 c_W^2}{\Lambda_2^3}. \quad (9)$$

在下面的讨论中, 为减少多余参数, 取  $k_1 = k_2 = 1$ .

此外, 算符

$$\mathcal{O}_{\text{FH}} = \frac{1}{\Lambda^3} \bar{\chi} \chi (D_\mu H)^\dagger D_\mu H \quad (10)$$

也会导致暗物质粒子与  $Z$  玻色子的相互作用. Higgs 场的协变导数可展开成

$$D_\mu H = (\partial_\mu - i g_1 B_\mu Y_H - i g_2 W_\mu^a T^a) H, \quad Y_H = \frac{1}{2}, \quad T^a = \frac{\sigma^a}{2}. \quad (11)$$

在么正规范下,  $H = \begin{pmatrix} \phi^+ \\ \phi^0 \end{pmatrix} \rightarrow \frac{1}{\sqrt{2}} \begin{pmatrix} 0 \\ v \end{pmatrix}$ , 而

$$W_\mu^a T^a \begin{pmatrix} 0 \\ v \end{pmatrix} = \frac{1}{2} \begin{pmatrix} W_\mu^3 & W_\mu^1 - i W_\mu^2 \\ W_\mu^1 + i W_\mu^2 & -W_\mu^3 \end{pmatrix} \begin{pmatrix} 0 \\ v \end{pmatrix} = \frac{1}{2} \begin{pmatrix} W_\mu^3 & \sqrt{2} W_\mu^+ \\ \sqrt{2} W_\mu^- & -W_\mu^3 \end{pmatrix} \begin{pmatrix} 0 \\ v \end{pmatrix} = \begin{pmatrix} \frac{1}{\sqrt{2}} W_\mu^+ v \\ -\frac{1}{2} W_\mu^3 v \end{pmatrix}, \quad (12)$$

其中  $W_\mu^\pm \equiv \frac{1}{\sqrt{2}}(W_\mu^1 \mp i W_\mu^2)$ , 则

$$\begin{aligned} (D_\mu H)^\dagger D^\mu H &\rightarrow \frac{v^2}{2} \left( \frac{1}{\sqrt{2}} g_2 W_\mu^-, \frac{1}{2} g_1 B_\mu - \frac{1}{2} g_2 W_\mu^3 \right) \begin{pmatrix} \frac{1}{\sqrt{2}} g_2 W^{+\mu} \\ \frac{1}{2} g_1 B^\mu - \frac{1}{2} g_2 W^{3\mu} \end{pmatrix} \\ &= \frac{1}{4} g_2^2 v^2 W^{+\mu} W_\mu^- + \frac{1}{8} (g_1^2 + g_2^2) v^2 Z_\mu Z^\mu = m_W^2 W^{+\mu} W_\mu^- + \frac{1}{2} m_Z^2 Z_\mu Z^\mu, \end{aligned} \quad (13)$$

其中  $Z_\mu \equiv \frac{1}{\sqrt{g_1^2 + g_2^2}}(g_2 W_\mu^3 - g_1 B_\mu)$ ,  $m_W \equiv \frac{1}{2} g_2 v$ ,  $m_Z \equiv \frac{1}{2} \sqrt{g_1^2 + g_2^2} v$ . 因此,

$$\mathcal{O}_{\text{FH}} \rightarrow \frac{1}{\Lambda^3} \bar{\chi} \chi (m_W^2 W^{+\mu} W_\mu^- + \frac{1}{2} m_Z^2 Z_\mu Z^\mu) = \frac{m_W^2}{\Lambda^3} \bar{\chi} \chi W^{+\mu} W_\mu^- + \frac{m_Z^2}{2\Lambda^3} \bar{\chi} \chi Z_\mu Z^\mu. \quad (14)$$

对于暗物质粒子与电子的耦合, 我们考虑有效算符

$$\mathcal{O}_{\text{FP}} = \frac{1}{\Lambda^2} \bar{\chi} \gamma_5 \chi \bar{e} \gamma_5 e, \quad \mathcal{O}_{\text{FA}} = \frac{1}{\Lambda^2} \bar{\chi} \gamma^\mu \gamma_5 \chi \bar{e} \gamma_\mu \gamma_5 e. \quad (15)$$

每一种算符对应于一个有效模型, 模型文件由 FeynRules 2 [3] 生成. 通过两体散射截面进行模型检验详见附录 A. MC 模拟由 MadGraph 5 [4], PYTHIA 6 [5] 和 PGS 4 [6] 完成.

参考 ILC TDR [7], 将电磁量能器和强子量能器的能量分辨分别假设为  $\frac{17\%}{\sqrt{E/\text{GeV}}} \oplus 1\%$  和  $\frac{30\%}{\sqrt{E/\text{GeV}}}$ .

对于信号, 取如下 benchmark points. 当  $\sqrt{s} = 250$  GeV 时,

$$\begin{aligned} \mathcal{O}_{\text{F1}} : \quad & \Lambda_1 = \Lambda_2 = 160 \text{ GeV}, \quad m_\chi = 25 \text{ GeV}, \quad \sigma = 71.5 \text{ fb}; \\ \mathcal{O}_{\text{F2}} : \quad & \Lambda_1 = \Lambda_2 = 120 \text{ GeV}, \quad m_\chi = 40 \text{ GeV}, \quad \sigma = 81.5 \text{ fb}; \\ \mathcal{O}_{\text{FH}} : \quad & \Lambda = 75 \text{ GeV}, \quad m_\chi = 2 \text{ GeV}, \quad \sigma = 73.3 \text{ fb}; \\ \mathcal{O}_{\text{FP}} : \quad & \Lambda = 110 \text{ GeV}, \quad m_\chi = 60 \text{ GeV}, \quad \sigma = 58.8 \text{ fb}; \\ \mathcal{O}_{\text{FA}} : \quad & \Lambda = 140 \text{ GeV}, \quad m_\chi = 50 \text{ GeV}, \quad \sigma = 71.2 \text{ fb}. \end{aligned} \quad (16)$$

当  $\sqrt{s} = 500$  GeV 时,

$$\begin{aligned} \mathcal{O}_{\text{F1}} : \quad & \Lambda_1 = \Lambda_2 = 280 \text{ GeV}, \quad m_\chi = 50 \text{ GeV}, \quad \sigma = 48.4 \text{ fb}; \\ \mathcal{O}_{\text{F2}} : \quad & \Lambda_1 = \Lambda_2 = 250 \text{ GeV}, \quad m_\chi = 80 \text{ GeV}, \quad \sigma = 53.4 \text{ fb}; \\ \mathcal{O}_{\text{FH}} : \quad & \Lambda = 100 \text{ GeV}, \quad m_\chi = 5 \text{ GeV}, \quad \sigma = 45.0 \text{ fb}; \\ \mathcal{O}_{\text{FP}} : \quad & \Lambda = 400 \text{ GeV}, \quad m_\chi = 120 \text{ GeV}, \quad \sigma = 58.6 \text{ fb}; \end{aligned}$$

$$\mathcal{O}_{\text{FA}} : \Lambda = 280 \text{ GeV}, \quad m_\chi = 150 \text{ GeV}, \quad \sigma = 50.2 \text{ fb}. \quad (17)$$

当  $\sqrt{s} = 1 \text{ TeV}$  时,

$$\begin{aligned} \mathcal{O}_{\text{F1}} : \Lambda_1 = \Lambda_2 = 440 \text{ GeV}, \quad m_\chi = 100 \text{ GeV}, \quad \sigma = 49.1 \text{ fb}; \\ \mathcal{O}_{\text{F2}} : \Lambda_1 = \Lambda_2 = 420 \text{ GeV}, \quad m_\chi = 160 \text{ GeV}, \quad \sigma = 52.6 \text{ fb}; \\ \mathcal{O}_{\text{FH}} : \Lambda = 120 \text{ GeV}, \quad m_\chi = 10 \text{ GeV}, \quad \sigma = 46.8 \text{ fb}; \\ \mathcal{O}_{\text{FP}} : \Lambda = 1000 \text{ GeV}, \quad m_\chi = 240 \text{ GeV}, \quad \sigma = 50.4 \text{ fb}; \\ \mathcal{O}_{\text{FA}} : \Lambda = 600 \text{ GeV}, \quad m_\chi = 300 \text{ GeV}, \quad \sigma = 55.0 \text{ fb}. \end{aligned} \quad (18)$$

## 2 轻子道

对于轻子衰变的  $Z$  玻色子,  $Z + \cancel{E}$  表现为  $\ell^+ \ell^- + \cancel{E}$ , 其中  $\ell = e, \mu$ . 主要背景为  $e^+ e^- \rightarrow \ell^+ \ell^- \bar{\nu} \nu$ ,  $e^+ e^- \rightarrow \tau^+ \tau^-$  和  $e^+ e^- \rightarrow \tau^+ \tau^- \bar{\nu} \nu$ .

当  $\sqrt{s} = 500 \text{ GeV}$  时, 事例筛选条件如下.

- **Cut 1:** 满足  $p_{\text{T}} > 10 \text{ GeV}$ ,  $|\eta| < 3$  的轻子有且只有 2 个, 并且它们异号同味 (opposite sign same flavor, OSSF). 没有  $p_{\text{T}} > 10 \text{ GeV}$ ,  $|\eta| < 3$  的 jet, 光子或  $\tau$ .
- **Cut 2:** 要求  $\cancel{E}_{\text{T}} > 30 \text{ GeV}$ .
- **Cut 3:** 要求两个轻子的不变质量  $m_{\ell\ell}$  满足  $|m_{\ell\ell} - m_Z| < 5 \text{ GeV}$ .
- **Cut 4:** 定义相对于两个轻子的反冲质量  $m_{\text{recoil}} = \sqrt{(p_{e^+} + p_{e^-} - p_{\ell_1} - p_{\ell_2})^2}$ , 其中  $p_{e^+}$  和  $p_{e^-}$  分别为束流正电子和电子的 4 动量. 除去  $m_{\text{recoil}} < 140 \text{ GeV}$  的事例.
- **Cut 5:** 要求两个轻子总动量的极角  $\theta_{\ell\ell}$  满足  $25^\circ < \theta_{\ell\ell} < 155^\circ$ .

$\sqrt{s} = 250 \text{ GeV}$  和  $1 \text{ TeV}$  时的事例筛选条件见 Tab. 1.

Table 1: 轻子道事例筛选条件.

	$\sqrt{s} = 250 \text{ GeV}$	$\sqrt{s} = 500 \text{ GeV}$	$\sqrt{s} = 1 \text{ TeV}$
Cut 1	2 OSSF leptons with $p_{\text{T}} > 10 \text{ GeV}$ , $ \eta  < 3$ no other particle or jet with $p_{\text{T}} > 10 \text{ GeV}$ , $ \eta  < 3$		
Cut 2	$\cancel{E}_{\text{T}} > 15 \text{ GeV}$	$\cancel{E}_{\text{T}} > 30 \text{ GeV}$	$\cancel{E}_{\text{T}} > 40 \text{ GeV}$
Cut 3	require $ m_{\ell\ell} - m_Z  < 5 \text{ GeV}$		
Cut 4	$m_{\text{recoil}} \geq 100 \text{ GeV}$	$m_{\text{recoil}} \geq 140 \text{ GeV}$	$m_{\text{recoil}} \geq 200 \text{ GeV}$
Cut 5	/	$25^\circ < \theta_{\ell\ell} < 155^\circ$	

信号和背景的分布如 Figs. 2, 3 和 4 所示.

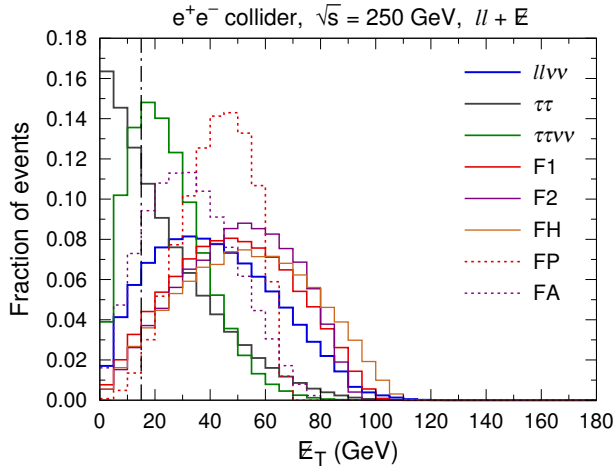
从运动学分析, 对于暗物质信号,  $\cancel{E}$  和  $\cancel{E}_{\text{T}}$  分布在

$$\frac{1}{2\sqrt{s}} \sqrt{[s - (2m_\chi + m_Z)^2][s - (2m_\chi - m_Z)^2]}$$

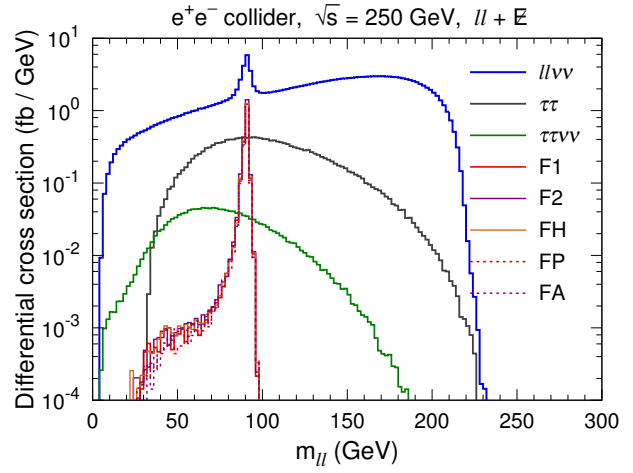
处会出现 endpoint, 而  $m_{\text{recoil}}$  分布在  $2m_\chi$  处会出现 endpoint.

经过事例筛选后, 背景与信号的截面及信号显著性如 Tab. 2 所示. 这里, 信号显著性定义是

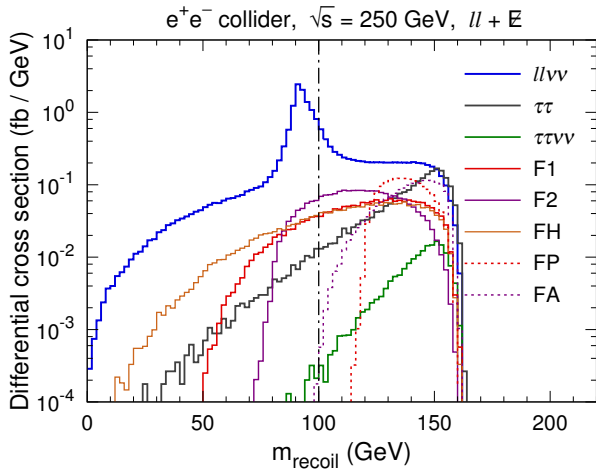
$$\mathcal{S} = \frac{S}{\sqrt{S+B}}. \quad (19)$$



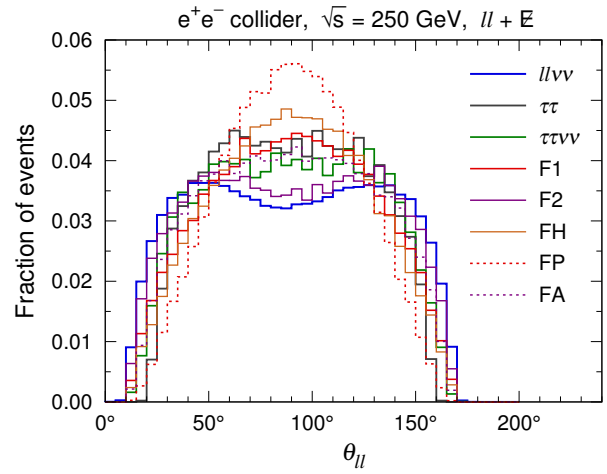
(a) 经过 Cut 1 之后, 归一化的  $E_T$  分布.



(b) 经过 Cut 2 之后, 关于  $m_{\ell\ell}$  的微分截面分布.

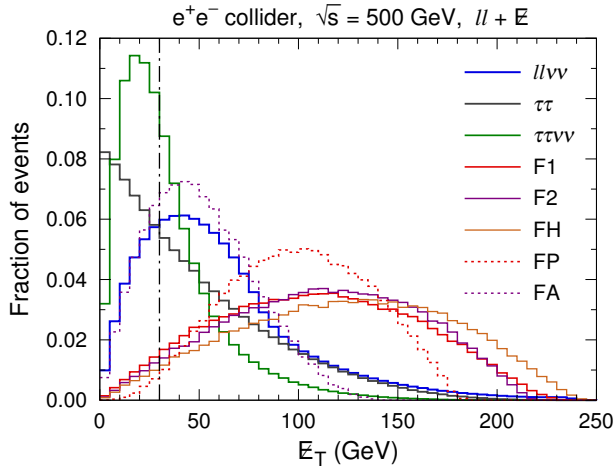


(c) 经过 Cut 3 之后, 关于  $m_{\text{recoil}}$  的微分截面分布.

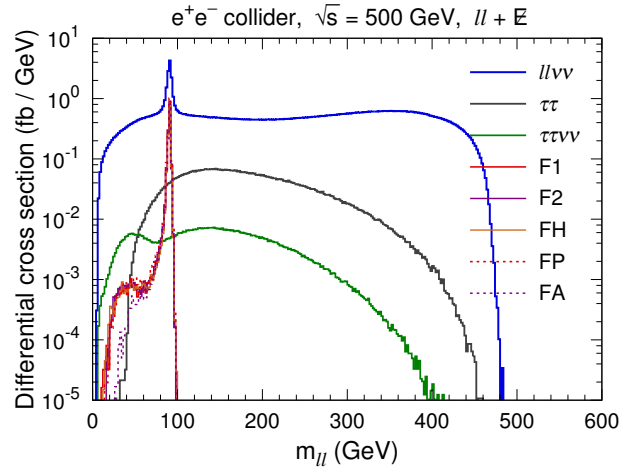


(d) 经过 Cut 4 之后, 归一化的  $\theta_{\ell\ell}$  分布.

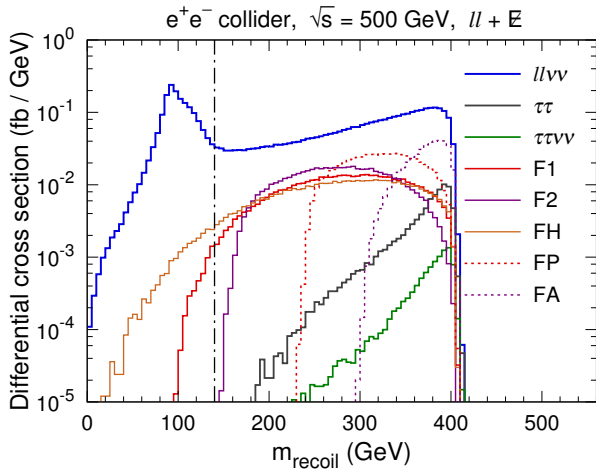
Figure 2:  $\sqrt{s} = 250$  GeV 时, 轻子道信号和背景分布. 点划线表示事例筛选条件的阈值.



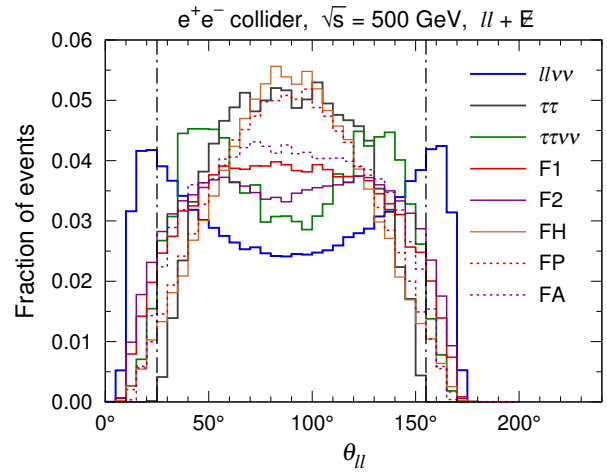
(a) 经过 Cut 1 之后, 归一化的  $E_T$  分布.



(b) 经过 Cut 2 之后, 关于  $m_{\ell\ell}$  的微分截面分布.

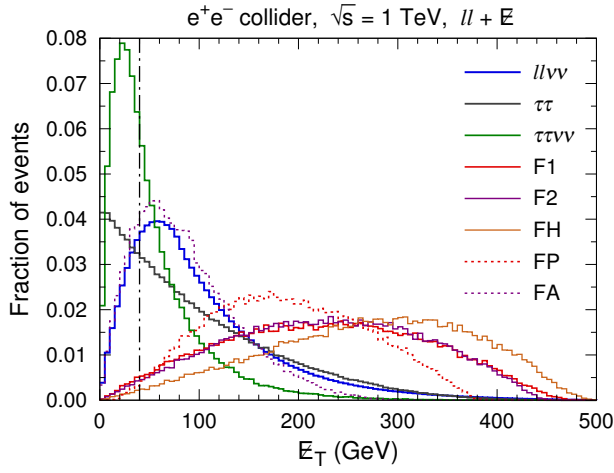


(c) 经过 Cut 3 之后, 关于  $m_{\text{recoil}}$  的微分截面分布.

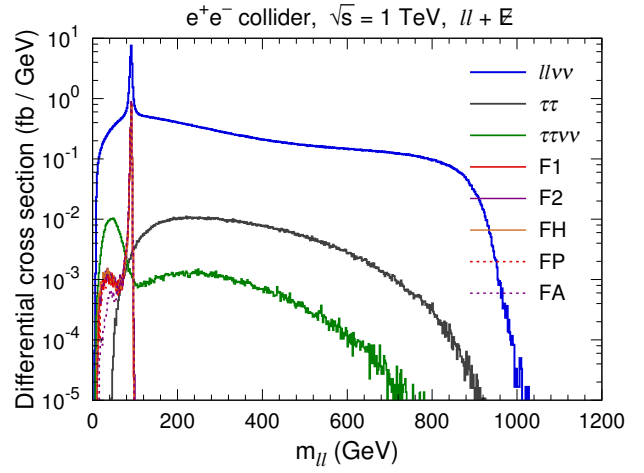


(d) 经过 Cut 4 之后, 归一化的  $\theta_{\ell\ell}$  分布.

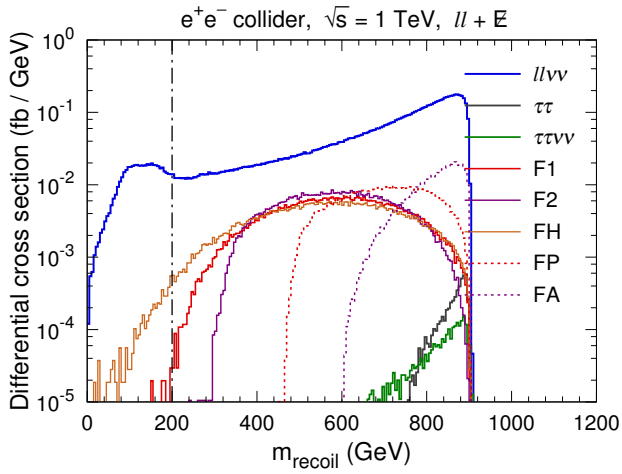
Figure 3:  $\sqrt{s} = 500$  GeV 时, 轻子道信号和背景分布. 点划线表示事例筛选条件的阈值.



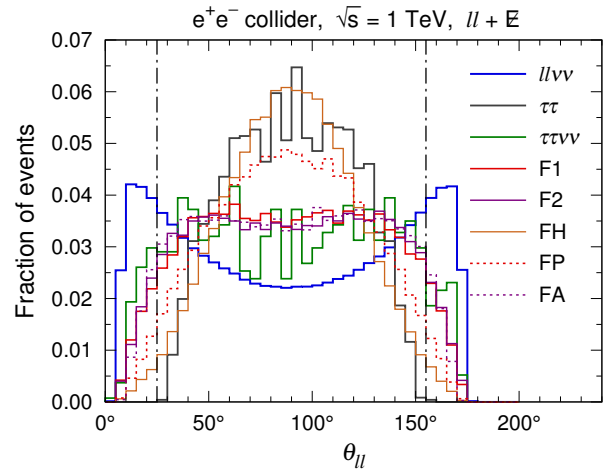
(a) 经过 Cut 1 之后, 归一化的  $E_T$  分布.



(b) 经过 Cut 2 之后, 关于  $m_{\ell\ell}$  的微分截面分布.



(c) 经过 Cut 3 之后, 关于  $m_{\text{recoil}}$  的微分截面分布.



(d) 经过 Cut 4 之后, 归一化的  $\theta_{\ell\ell}$  分布.

Figure 4:  $\sqrt{s} = 1$  TeV 时, 轻子道信号和背景的分布. 点划线表示事例筛选条件的阈值.

Table 2: 经过每次事例筛选后, 轻子道背景与信号的截面及信号显著性.

$\sqrt{s} = 250 \text{ GeV}$													
	$\ell^+\ell^-\bar{\nu}\nu$	$\tau^+\tau^-$	$\tau^+\tau^-\bar{\nu}\nu$	$\mathcal{O}_{F1}$		$\mathcal{O}_{F2}$		$\mathcal{O}_{FH}$		$\mathcal{O}_{FP}$		$\mathcal{O}_{FA}$	
	$\sigma$	$\sigma$	$\sigma$	$\sigma$	$\mathcal{S}$	$\sigma$	$\mathcal{S}$	$\sigma$	$\mathcal{S}$	$\sigma$	$\mathcal{S}$	$\sigma$	$\mathcal{S}$
Cut 1	425	62.1	4.36	4.08	1.84	4.65	2.09	4.15	1.87	3.38	1.52	4.12	1.85
Cut 2	376	35.1	3.15	3.84	1.88	4.44	2.17	3.95	1.93	3.31	1.62	3.56	1.74
Cut 3	36.8	4.24	0.342	3.65	5.44	4.23	6.27	3.77	5.62	3.16	4.74	3.39	5.07
Cut 4	13.0	4.03	0.339	2.93	6.50	3.46	7.58	2.71	6.04	3.16	6.97	3.39	7.44

$\sqrt{s} = 500 \text{ GeV}$													
	$\ell^+\ell^-\bar{\nu}\nu$	$\tau^+\tau^-$	$\tau^+\tau^-\bar{\nu}\nu$	$\mathcal{O}_{F1}$		$\mathcal{O}_{F2}$		$\mathcal{O}_{FH}$		$\mathcal{O}_{FP}$		$\mathcal{O}_{FA}$	
	$\sigma$	$\sigma$	$\sigma$	$\sigma$	$\mathcal{S}$	$\sigma$	$\mathcal{S}$	$\sigma$	$\mathcal{S}$	$\sigma$	$\mathcal{S}$	$\sigma$	$\mathcal{S}$
Cut 1	306	20.4	2.85	2.65	1.46	2.94	1.61	2.47	1.36	3.24	1.78	2.86	1.57
Cut 2	235	11.8	1.29	2.52	1.60	2.82	1.78	2.39	1.51	3.19	2.01	2.19	1.38
Cut 3	23.9	0.410	0.0495	2.41	4.67	2.70	5.18	2.29	4.44	3.06	5.84	2.09	4.07
Cut 4	16.0	0.410	0.0495	2.39	5.51	2.70	6.16	2.19	5.08	3.06	6.92	2.09	4.86
Cut 5	12.1	0.410	0.0471	2.19	5.69	2.42	6.24	2.11	5.50	2.95	7.47	2.01	5.25

$\sqrt{s} = 1 \text{ TeV}$													
	$\ell^+\ell^-\bar{\nu}\nu$	$\tau^+\tau^-$	$\tau^+\tau^-\bar{\nu}\nu$	$\mathcal{O}_{F1}$		$\mathcal{O}_{F2}$		$\mathcal{O}_{FH}$		$\mathcal{O}_{FP}$		$\mathcal{O}_{FA}$	
	$\sigma$	$\sigma$	$\sigma$	$\sigma$	$\mathcal{S}$	$\sigma$	$\mathcal{S}$	$\sigma$	$\mathcal{S}$	$\sigma$	$\mathcal{S}$	$\sigma$	$\mathcal{S}$
Cut 1	297	5.84	1.74	2.69	1.54	2.92	1.67	2.58	1.47	2.77	1.58	3.06	1.74
Cut 2	245	4.10	0.854	2.64	1.66	2.87	1.80	2.55	1.61	2.74	1.72	2.47	1.55
Cut 3	40.0	0.0257	0.0122	2.53	3.87	2.75	4.20	2.44	3.75	2.63	4.02	2.37	3.64
Cut 4	37.6	0.0257	0.0122	2.53	3.99	2.75	4.32	2.42	3.82	2.63	4.14	2.37	3.74
Cut 5	26.5	0.0256	0.0104	2.25	4.19	2.44	4.53	2.36	4.39	2.49	4.63	2.12	3.97

截面  $\sigma$  的单位为 fb. 信号显著性定义为  $\mathcal{S} = S/\sqrt{S+B}$ , 对应于  $100 \text{ fb}^{-1}$ .



### 3 强子道

对于强子衰变的  $Z$  玻色子,  $Z + \cancel{E}$  表现为  $jj + \cancel{E}$ . 主要背景为  $e^+e^- \rightarrow jj\nu\bar{\nu}$ ,  $e^+e^- \rightarrow jj\ell\nu$  和  $e^+e^- \rightarrow t\bar{t}$ . 当  $\sqrt{s} = 500$  GeV 时, 事例筛选条件如下.

- **Cut 1:** 满足  $p_T > 10$  GeV,  $|\eta| < 3$  的 jet 有且只有 2 个. 没有  $p_T > 10$  GeV,  $|\eta| < 3$  的  $e, \mu, \tau$  或光子.
- **Cut 2:** 要求  $\cancel{E}_T > 30$  GeV.
- **Cut 3:** 要求两个 jet 的不变质量  $m_{jj}$  满足  $40 \text{ GeV} < m_{jj} < 95 \text{ GeV}$ .
- **Cut 4:** 定义相对于两个 jet 的反冲质量  $m_{\text{recoil}} = \sqrt{(p_{e^+} + p_{e^-} - p_{j_1} - p_{j_2})^2}$ , 其中  $p_{e^+}$  和  $p_{e^-}$  分别为束流正电子和电子的 4 动量. 除去  $m_{\text{recoil}} < 200$  GeV 的事例.
- **Cut 5:** 要求两个 jet 总动量的极角  $\theta_{jj}$  满足  $25^\circ < \theta_{jj} < 155^\circ$ .

$\sqrt{s} = 250$  GeV 和 1 TeV 时的事例筛选条件见 Tab. 3.

Table 3: 强子道事例筛选条件.

	$\sqrt{s} = 250 \text{ GeV}$	$\sqrt{s} = 500 \text{ GeV}$	$\sqrt{s} = 1 \text{ TeV}$
Cut 1	exact 2 jets with $p_T > 10 \text{ GeV}$ , $ \eta  < 3$ no other particle with $p_T > 10 \text{ GeV}$ , $ \eta  < 3$		
Cut 2	$\cancel{E}_T > 15 \text{ GeV}$	$\cancel{E}_T > 30 \text{ GeV}$	$\cancel{E}_T > 40 \text{ GeV}$
Cut 3	$50 \text{ GeV} < m_{jj} < 95 \text{ GeV}$	$40 \text{ GeV} < m_{jj} < 95 \text{ GeV}$	
Cut 4	$m_{\text{recoil}} \geq 120 \text{ GeV}$	$m_{\text{recoil}} \geq 200 \text{ GeV}$	$m_{\text{recoil}} \geq 300 \text{ GeV}$
Cut 5	$30^\circ < \theta_{jj} < 150^\circ$	$25^\circ < \theta_{jj} < 155^\circ$	

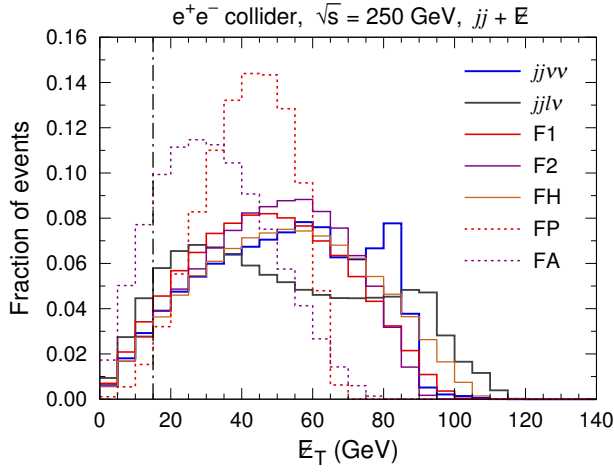
信号和背景的分布如 Fig. 5, 6 和 7 所示. 在  $m_{jj}$  分布中,  $jj\nu\bar{\nu}$  过程在  $\sim 120$  GeV 附近的峰来自于 Higgs 玻色子的强子衰变道.

与轻子道一样, 对于暗物质信号,  $\cancel{E}$  和  $\cancel{E}_T$  分布在

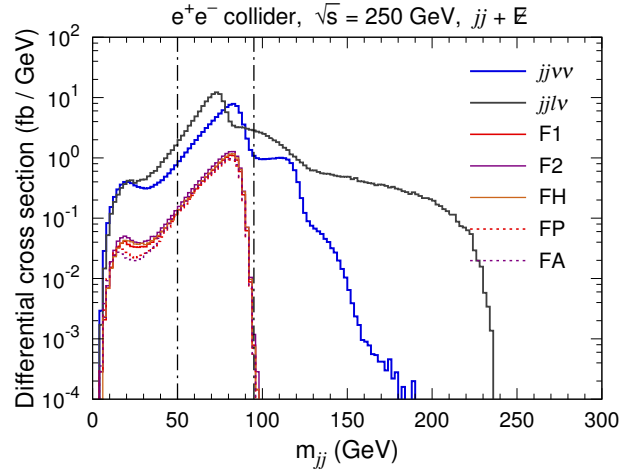
$$\frac{1}{2\sqrt{s}} \sqrt{[s - (2m_\chi + m_Z)^2][s - (2m_\chi - m_Z)^2]}$$

处会出现 endpoint,  $m_{\text{recoil}}$  分布在  $2m_\chi$  处会出现 endpoint.

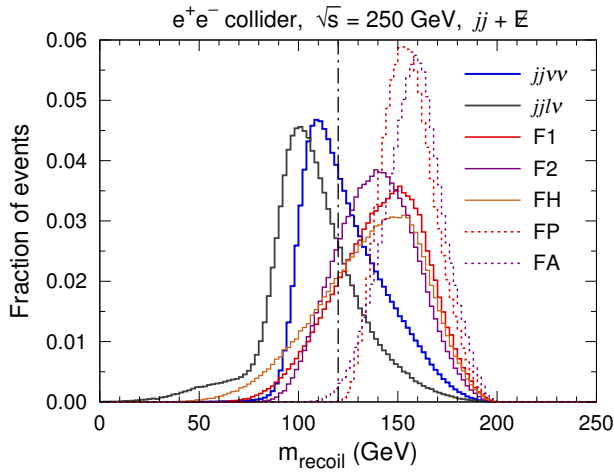
经过事例筛选后, 背景与信号的截面及信号显著性如 Tab. 4 所示.



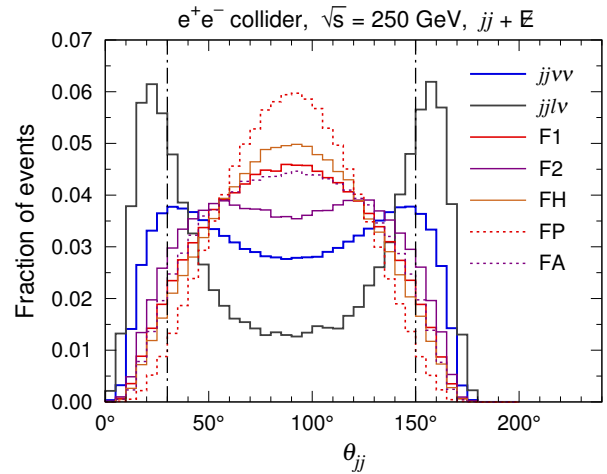
(a) 经过 Cut 1 之后, 归一化的  $E_T$  分布.



(b) 经过 Cut 2 之后, 关于  $m_{jj}$  的微分截面分布.

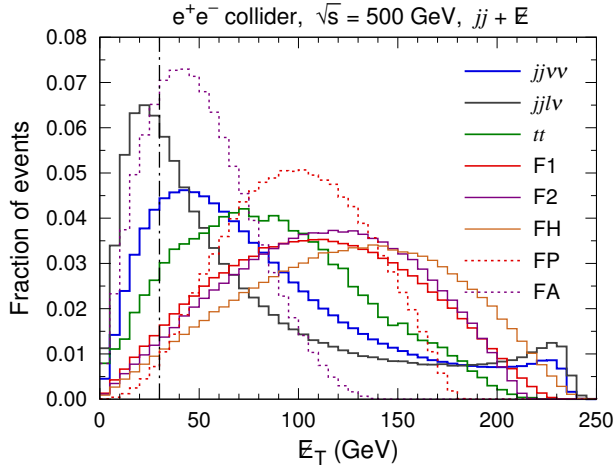


(c) 经过 Cut 3 之后, 归一化的  $m_{\text{recoil}}$  分布.

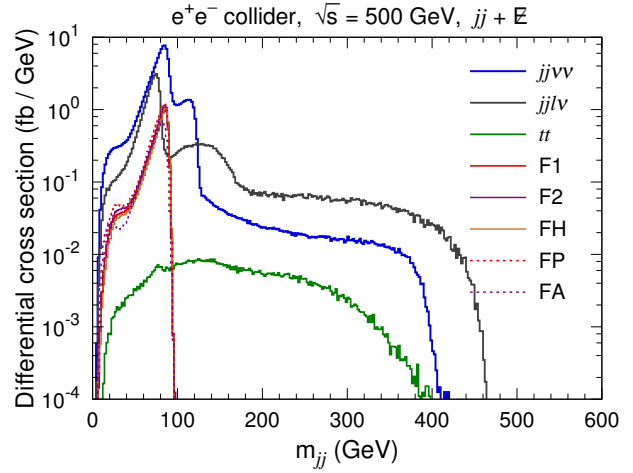


(d) 经过 Cut 4 之后, 归一化的  $\theta_{jj}$  分布.

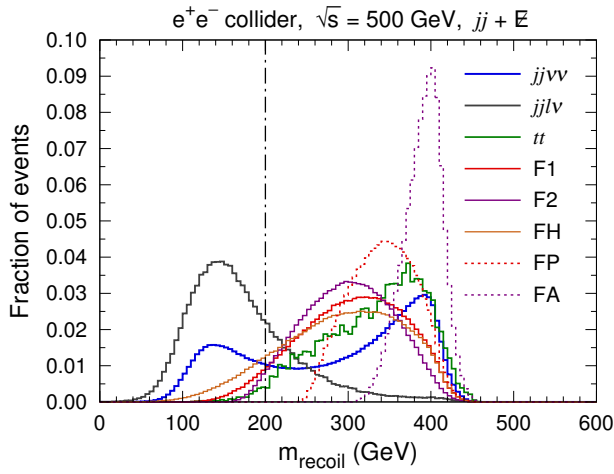
Figure 5:  $\sqrt{s} = 250$  GeV 时, 强子道信号和背景分布. 点划线表示事例筛选条件的阈值.



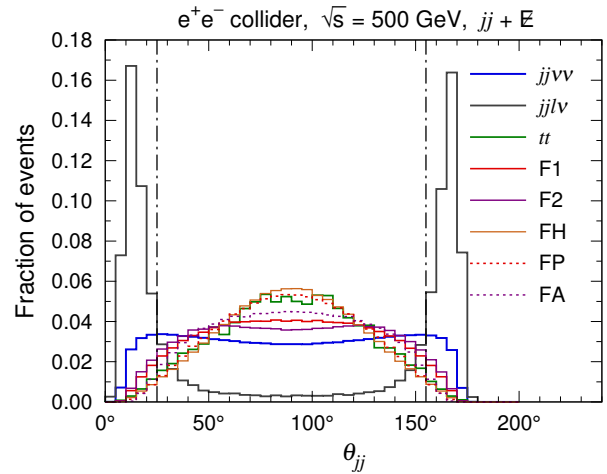
(a) 经过 Cut 1 之后, 归一化的  $E_T$  分布.



(b) 经过 Cut 2 之后, 关于  $m_{jj}$  的微分截面分布.

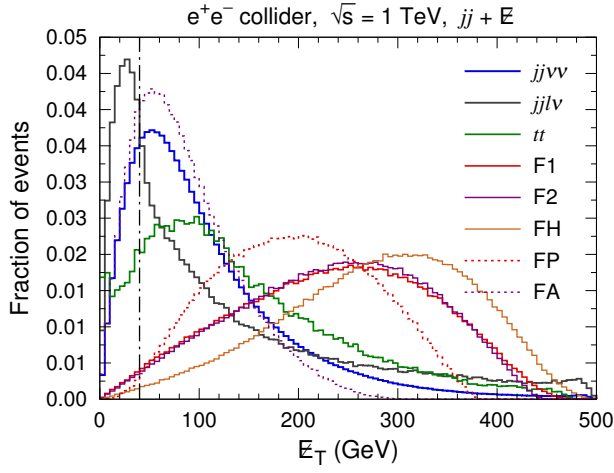


(c) 经过 Cut 3 之后, 归一化的  $m_{recoil}$  分布.

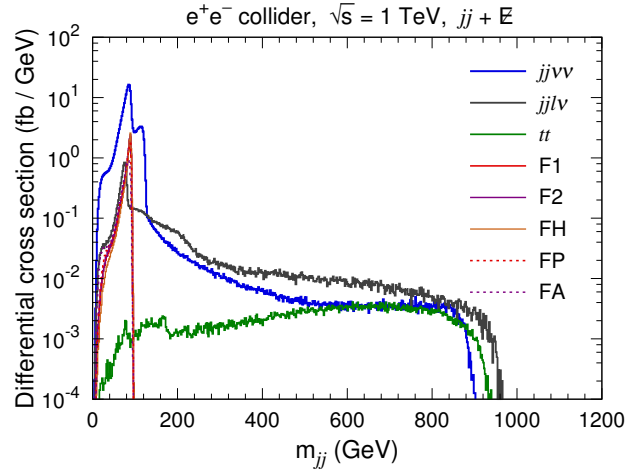


(d) 经过 Cut 4 之后, 归一化的  $\theta_{jj}$  分布.

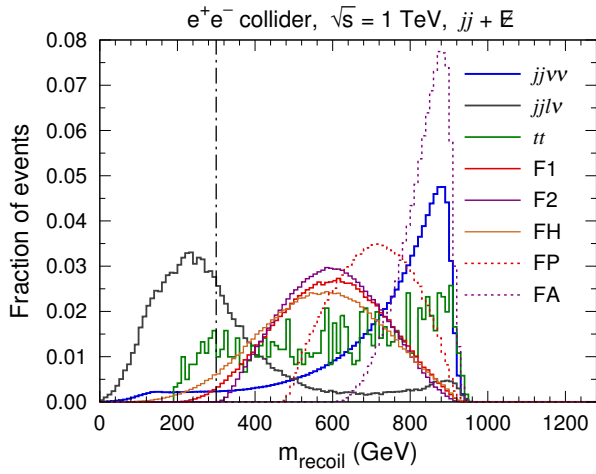
Figure 6:  $\sqrt{s} = 500$  GeV 时, 强子道信号和背景分布. 点划线表示事例筛选条件的阈值.



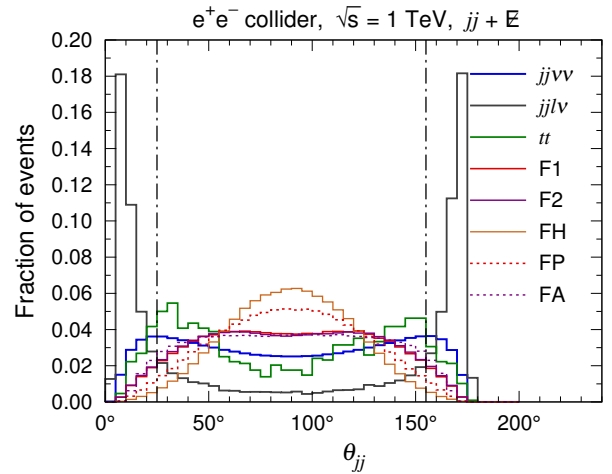
(a) 经过 Cut 1 之后, 归一化的  $E_T$  分布.



(b) 经过 Cut 2 之后, 关于  $m_{jj}$  的微分截面分布.



(c) 经过 Cut 3 之后, 归一化的  $m_{recoil}$  分布.



(d) 经过 Cut 4 之后, 归一化的  $\theta_{jj}$  分布.

Figure 7:  $\sqrt{s} = 1$  TeV 时, 强子道信号和背景的分布. 点划线表示事例筛选条件的阈值.

Table 4: 经过每次事例筛选后, 强子道背景与信号的截面及信号显著性.

$\sqrt{s} = 250 \text{ GeV}$													
	$jj\nu\bar{\nu}$	$jj\ell\nu$	$\mathcal{O}_{F1}$		$\mathcal{O}_{F2}$		$\mathcal{O}_{FH}$		$\mathcal{O}_{FP}$		$\mathcal{O}_{FA}$		
	$\sigma$	$\sigma$	$\sigma$	$\mathcal{S}$	$\sigma$	$\mathcal{S}$	$\sigma$	$\mathcal{S}$	$\sigma$	$\mathcal{S}$	$\sigma$	$\mathcal{S}$	
Cut 1	220	393	26.0	10.3	29.7	11.7	26.7	10.6	21.3	8.45	25.8	10.2	
Cut 2	208	361	24.4	10.0	28.2	11.6	25.4	10.4	20.8	8.57	22.1	9.08	
Cut 3	167	251	22.5	10.7	26.0	12.3	23.4	11.1	19.2	9.19	20.4	9.76	
Cut 4	82.6	63.8	18.5	14.4	21.4	16.5	17.3	13.5	19.2	14.9	20.3	15.7	
Cut 5	63.8	34.6	16.8	15.6	18.6	17.2	16.0	14.9	18.5	17.1	18.5	17.1	

$\sqrt{s} = 500 \text{ GeV}$													
	$jj\nu\bar{\nu}$	$jj\ell\nu$	$t\bar{t}$	$\mathcal{O}_{F1}$		$\mathcal{O}_{F2}$		$\mathcal{O}_{FH}$		$\mathcal{O}_{FP}$		$\mathcal{O}_{FA}$	
	$\sigma$	$\sigma$	$\sigma$	$\sigma$	$\mathcal{S}$	$\sigma$	$\mathcal{S}$	$\sigma$	$\mathcal{S}$	$\sigma$	$\mathcal{S}$	$\sigma$	$\mathcal{S}$
Cut 1	245	131	1.74	18.9	9.47	20.9	10.4	17.8	8.94	22.1	11.1	18.4	9.24
Cut 2	207	93.2	1.56	18.0	10.0	20.0	11.2	17.2	9.64	21.8	12.1	13.9	7.84
Cut 3	160	56.6	0.270	17.2	11.2	19.2	12.5	16.6	10.8	20.7	13.5	13.3	8.76
Cut 4	115	14.9	0.264	16.3	13.4	18.7	15.3	14.6	12.1	20.7	16.9	13.3	11.1
Cut 5	92.6	2.91	0.253	15.1	14.3	17.1	16.1	14.1	13.5	20.1	18.7	12.9	12.3

$\sqrt{s} = 1 \text{ TeV}$													
	$jj\nu\bar{\nu}$	$jj\ell\nu$	$t\bar{t}$	$\mathcal{O}_{F1}$		$\mathcal{O}_{F2}$		$\mathcal{O}_{FH}$		$\mathcal{O}_{FP}$		$\mathcal{O}_{FA}$	
	$\sigma$	$\sigma$	$\sigma$	$\sigma$	$\mathcal{S}$	$\sigma$	$\mathcal{S}$	$\sigma$	$\mathcal{S}$	$\sigma$	$\mathcal{S}$	$\sigma$	$\mathcal{S}$
Cut 1	511	49.1	0.951	24.3	10.0	26.1	10.8	24.0	9.92	23.0	9.50	21.0	8.72
Cut 2	421	34.4	0.824	23.9	10.9	25.7	11.7	23.9	10.9	22.8	10.4	17.1	7.84
Cut 3	318	15.2	0.0201	23.5	12.4	25.3	13.4	23.6	12.5	22.3	11.8	16.3	8.71
Cut 4	303	6.07	0.0180	23.3	12.8	25.3	13.8	22.6	12.4	22.3	12.2	16.3	9.02
Cut 5	234	1.43	0.0147	21.2	13.2	23.0	14.3	22.1	13.8	21.4	13.3	14.8	9.37

截面  $\sigma$  的单位为 fb. 信号显著性定义为  $\mathcal{S} = S/\sqrt{S+B}$ , 对应于  $100 \text{ fb}^{-1}$ .

## 4 实验灵敏度

Fig. 8 展示了由  $\mathcal{S} = 3$  给出的  $3\sigma$  实验灵敏度曲线. 这里假设收集的数据量为  $1000 \text{ fb}^{-1}$ . 对于算符  $\mathcal{O}_{F1}$  和  $\mathcal{O}_{F2}$ , 均假设  $\Lambda_1 = \Lambda_2$ . 将  $3\sigma$  灵敏度曲线转换到湮灭截面与暗物质粒子质量的平面上的结果见 Fig. 9. 湮灭截面公式见 (63) 和 (81).

由于算符  $\mathcal{O}_{F1}$  和  $\mathcal{O}_{F2}$  各有两个 cutoff 参数, 参数间不同关系会影响截面大小 (参考附录 B). 上面所取的  $\Lambda_1 = \Lambda_2$  恰好关掉了  $\chi\chi\gamma Z$  耦合  $G_{AZ}$ . 若  $\Lambda_1 = -\Lambda_2$ , 则  $\chi\chi\gamma Z$  耦合会给出比较显著的贡献.  $\sqrt{s} = 500 \text{ GeV}$  时, 在不同参数关系下的实验灵敏度如 Fig. 10 所示.

## 5 极化束流

极化的束流对于背景和信号的产生截面有着不同的影响, 参见附录 C. 根据 ILC 的 TDR [9], 可以达得的束流极化度范围为

$$-0.8 \leq P_{e-} \leq +0.8, \quad -0.3 \leq P_{e+} \leq +0.3. \quad (20)$$

取不同的束流极化度, 经过事例筛选 (Cut 5) 后, 主要背景与信号的可见截面 (单位为 fb) 如 Tab. 5 所示.

Table 5: 在不同的束流极化度构型下, 经过事例筛选 (Cut 5) 后主要背景与信号的截面 (单位为 fb).

$\sqrt{s} = 500 \text{ GeV}$ , 轻子道							
$(P_{e-}, P_{e+})$	$\ell^+\ell^-\bar{\nu}\nu$	$\mathcal{O}_{F1}$	$\mathcal{O}_{F2}$	$\mathcal{O}_{FH}$	$\mathcal{O}_{FP}$	$\mathcal{O}_{FA}$	
(0, 0)	12.1	2.19	2.42	2.11	2.95	2.01	
(+0.8, -0.3)	2.02	2.19	2.43	2.08	2.24	1.97	
(+0.8, +0.3)	3.48	1.42	1.56	1.40	3.63	1.30	
(-0.8, -0.3)	15.2	1.89	2.09	1.82	3.63	1.75	
(-0.8, +0.3)	27.6	3.24	3.59	3.13	2.24	3.02	

$\sqrt{s} = 500 \text{ GeV}$ , 强子道							
$(P_{e-}, P_{e+})$	$jj\nu\bar{\nu}$	$jj\ell\nu$	$\mathcal{O}_{F1}$	$\mathcal{O}_{F2}$	$\mathcal{O}_{FH}$	$\mathcal{O}_{FP}$	$\mathcal{O}_{FA}$
(0, 0)	92.6	2.91	15.1	17.1	14.1	20.1	12.9
(+0.8, -0.3)	17.4	0.776	15.0	17.0	14.2	15.2	12.8
(+0.8, +0.3)	26.2	1.07	9.77	11.2	9.17	24.9	8.40
(-0.8, -0.3)	115	3.85	13.1	14.8	12.2	24.9	11.2
(-0.8, +0.3)	212	6.05	22.3	25.3	20.9	15.2	19.0

电子与  $Z$  玻色子的耦合项为

$$\frac{g_2}{2c_W}(g_L\bar{\ell}_L\gamma^\mu\ell_L + g_R\bar{\ell}_R\gamma^\mu\ell_R)Z_\mu, \quad (21)$$

其中,

$$g_L = -1 + 2s_W^2 = -0.555507, \quad g_R = 2s_W^2 = 0.444493, \quad \frac{g_L^2}{g_R^2} = 1.56. \quad (22)$$

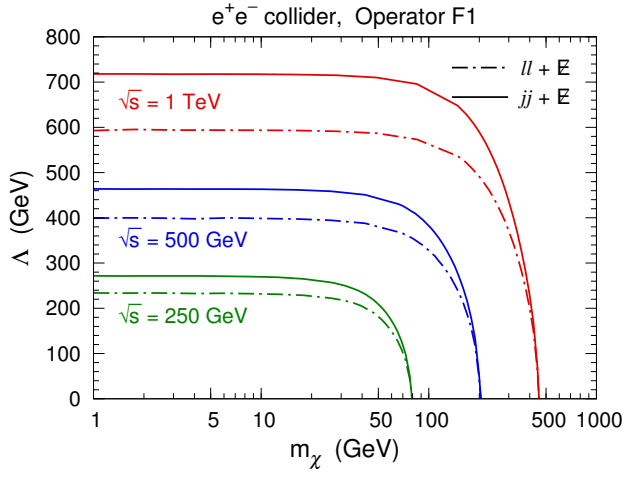
因此, 左手电子 (右手正电子) 与  $Z$  玻色子的耦合更强. 另外,  $W$  玻色子只与左手电子 (右手正电子) 耦合. 由于这些原因, 对于背景  $\ell^+\ell^-\bar{\nu}\nu$ ,  $jj\nu\bar{\nu}$  和  $jj\ell\nu$ ,  $(P_{e-}, P_{e+}) = (+0.8, -0.3)$  时压低得最好,  $(P_{e-}, P_{e+}) = (+0.8, +0.3)$  次之.

由于

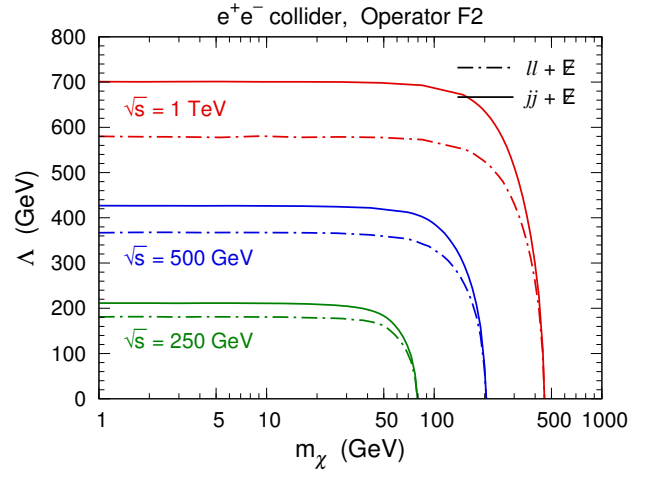
$$\bar{\psi}\gamma^\mu\psi = \bar{\psi}_L\gamma^\mu\psi_L + \bar{\psi}_R\gamma^\mu\psi_R, \quad \bar{\psi}\gamma^\mu\gamma_5\psi = \bar{\psi}_L\gamma^\mu\gamma_5\psi_L + \bar{\psi}_R\gamma^\mu\gamma_5\psi_R, \quad (23)$$

$$\bar{\psi}\psi = \bar{\psi}_L\psi_R + \bar{\psi}_R\psi_L, \quad \bar{\psi}i\gamma_5\psi = \bar{\psi}_Li\gamma_5\psi_R + \bar{\psi}_Ri\gamma_5\psi_L = i\bar{\psi}_L\psi_R - i\bar{\psi}_R\psi_L, \quad (24)$$

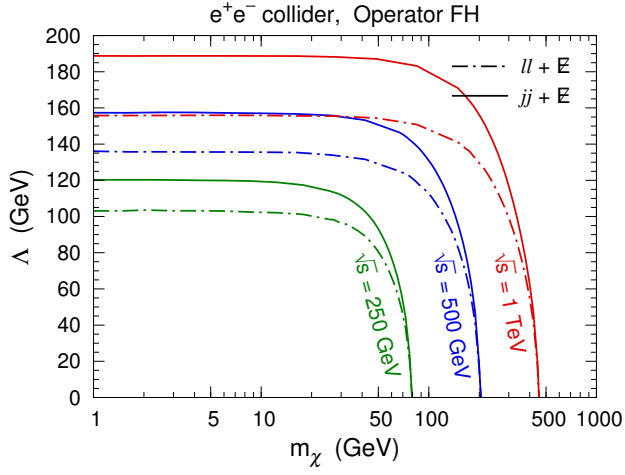
$$\bar{\psi}\sigma^{\mu\nu}\psi = \bar{\psi}_L\sigma^{\mu\nu}\psi_R + \bar{\psi}_R\sigma^{\mu\nu}\psi_L, \quad (25)$$



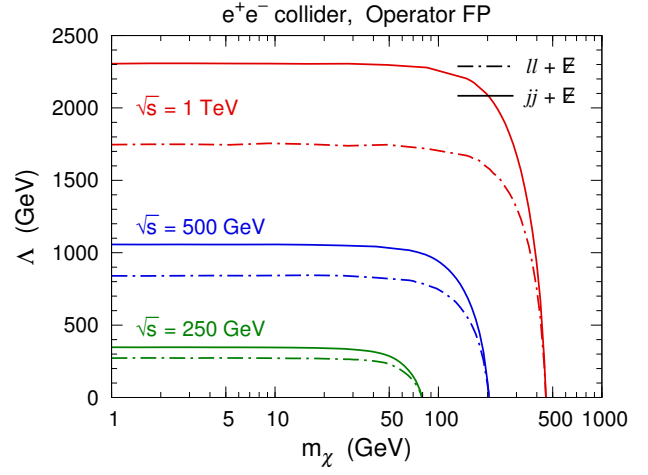
(a) 算符  $\mathcal{O}_{F1}$ ,  $\Lambda = \Lambda_1 = \Lambda_2$ .



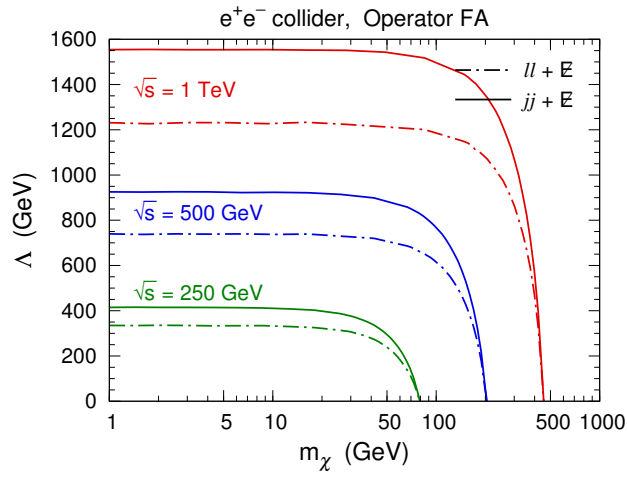
(b) 算符  $\mathcal{O}_{F2}$ ,  $\Lambda = \Lambda_1 = \Lambda_2$ .



(c) 算符  $\mathcal{O}_{FH}$ .

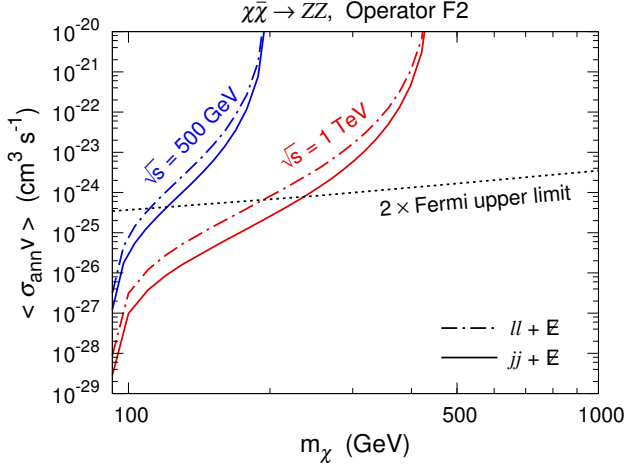


(d) 算符  $\mathcal{O}_{FP}$ .

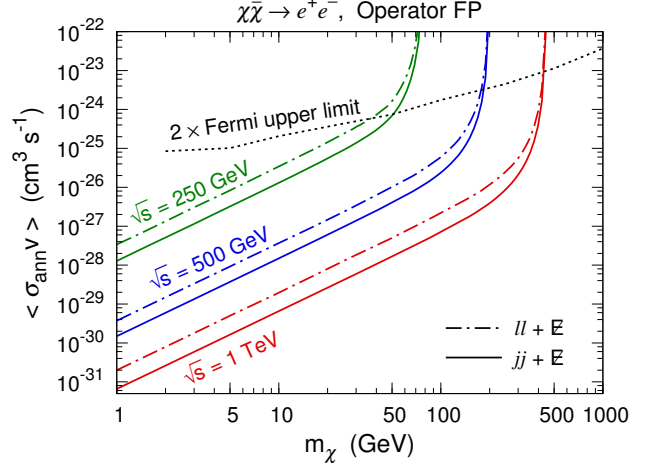


(e) 算符  $\mathcal{O}_{FA}$ .

Figure 8:  $3\sigma$  的实验灵敏度曲线. 这里假设积分亮度为  $1000 \text{ fb}^{-1}$ .

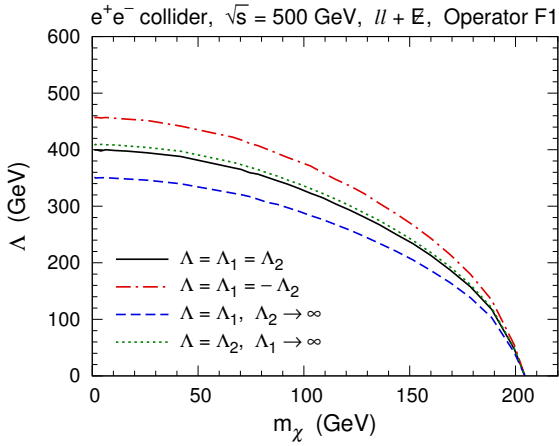


(a) 算符  $\mathcal{O}_{F2}$ ,  $\Lambda_1 = \Lambda_2$ , 暗物质湮灭到  $ZZ$ .

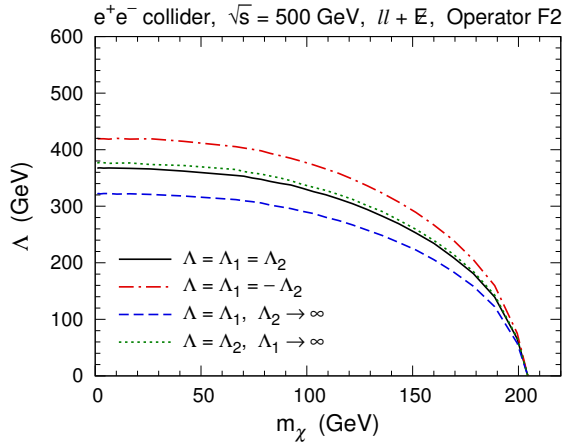


(b) 算符  $\mathcal{O}_{FP}$ , 暗物质湮灭到  $e^+e^-$ .

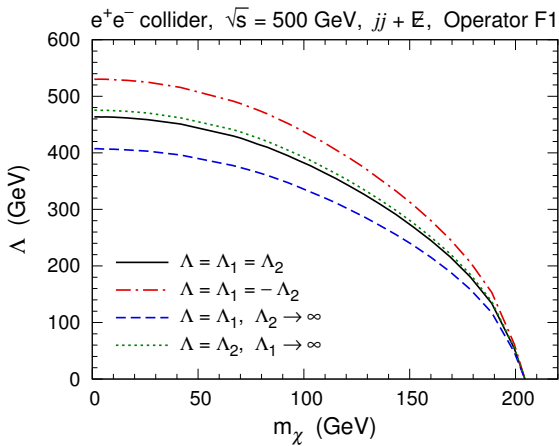
Figure 9: 在湮灭截面与暗物质粒子质量的平面上,  $3\sigma$  的实验灵敏度曲线. 这里假设积分亮度为  $1000 \text{ fb}^{-1}$ . 实线对应于强子道, 点划线对于轻子道. 点线代表 Fermi-LAT 通过对矮星系的伽马射线观测所给出的上限 [8].



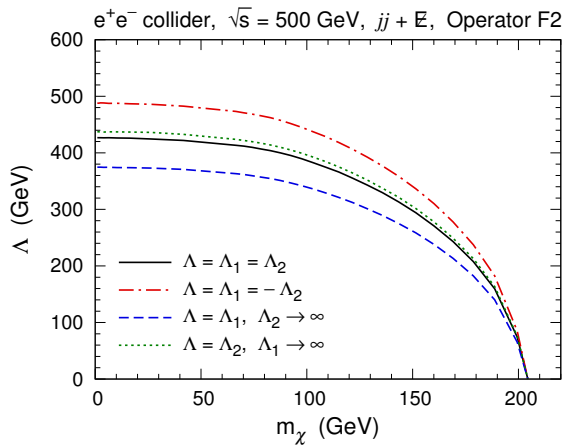
(a) 轻子道, 算符  $\mathcal{O}_{F1}$ .



(b) 轻子道, 算符  $\mathcal{O}_{F2}$ .



(c) 强子道, 算符  $\mathcal{O}_{F1}$ .



(d) 强子道, 算符  $\mathcal{O}_{F2}$ .

Figure 10:  $\sqrt{s} = 500 \text{ GeV}$  时, 不同参数关系下的实验灵敏度. 这里假设积分亮度为  $1000 \text{ fb}^{-1}$ .

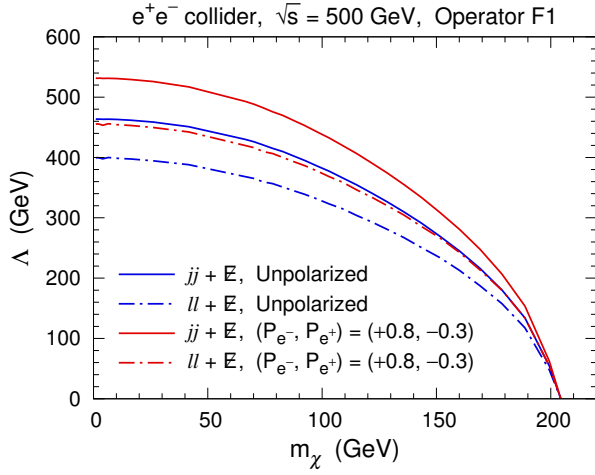


Table 6: 非极化束流与优化的极化束流对应的信号显著性  $S$  (积分亮度为  $100 \text{ fb}^{-1}$ ).

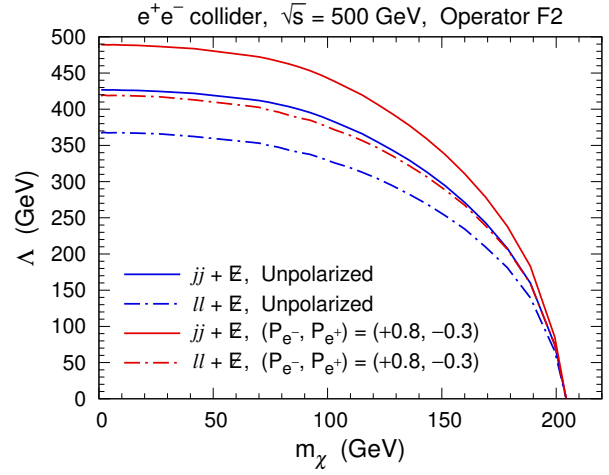
$\sqrt{s} = 500 \text{ GeV}$ , 轻子道				$\sqrt{s} = 500 \text{ GeV}$ , 强子道			
	$\mathcal{S}_{\text{unpol}}$	$\mathcal{S}_{\text{pol}}$	$\mathcal{S}_{\text{pol}}/\mathcal{S}_{\text{unpol}}$		$\mathcal{S}_{\text{unpol}}$	$\mathcal{S}_{\text{pol}}$	$\mathcal{S}_{\text{pol}}/\mathcal{S}_{\text{unpol}}$
$\mathcal{O}_{\text{F1}}$	5.69	10.1	1.78	$\mathcal{O}_{\text{F1}}$	14.3	26.0	1.82
$\mathcal{O}_{\text{F2}}$	6.24	10.9	1.75	$\mathcal{O}_{\text{F2}}$	16.1	28.6	1.78
$\mathcal{O}_{\text{FH}}$	5.50	9.70	1.76	$\mathcal{O}_{\text{FH}}$	13.5	24.8	1.84
$\mathcal{O}_{\text{FP}}$	7.47	13.4	1.79	$\mathcal{O}_{\text{FP}}$	18.7	34.4	1.84
$\mathcal{O}_{\text{FA}}$	5.25	9.29	1.77	$\mathcal{O}_{\text{FA}}$	12.3	23.0	1.87

$\mathcal{S}_{\text{unpol}}$  和  $\mathcal{S}_{\text{pol}}$  分别对应于非极化束流和优化的极化束流.

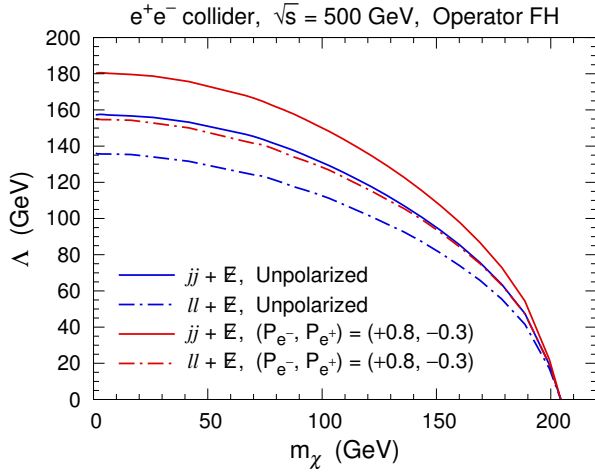
费米子的矢量流和轴矢量流耦合导致湮灭成矢量粒子的电子和正电子螺旋度必须相反, 而辐射出矢量粒子的电子或正电子螺旋度与辐射之前相同. 另一方面, 费米子的标量、赝标量和二阶张量耦合要求进行  $s$ -channel 湮灭的电子和正电子螺旋度相同. 因此, 对于算符  $\mathcal{O}_{\text{F1}}$ ,  $\mathcal{O}_{\text{F2}}$ ,  $\mathcal{O}_{\text{FH}}$  和  $\mathcal{O}_{\text{FA}}$ , 需要束流电子与正电子的螺旋度相反 (矢量流或轴矢量流), 才有非零的截面, 故在  $(P_{e^-}, P_{e^+}) = (+0.8, -0.3)$  时可以得到最好的信号显著性. 而对于算符  $\mathcal{O}_{\text{FP}}$ , 则需要束流电子与正电子的螺旋度相同 (赝标量相互作用), 才有非零的截面, 故在  $(P_{e^-}, P_{e^+}) = (+0.8, +0.3)$  时得到最好的信号显著性. 非极化束流与优化的极化束流对应的信号显著性如 Table. 6 所示. 可见, 使用优化的极化束流相当于收集到的数据量为原来的 3 倍多. 用优化的极化束流给出的  $3\sigma$  实验灵敏度曲线如 Fig. 11 所示.



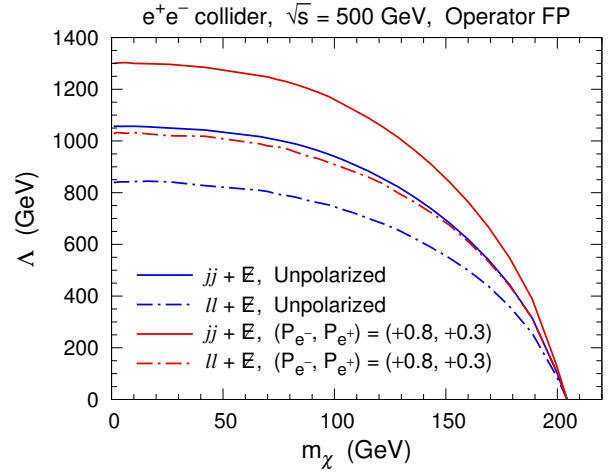
(a) 算符  $\mathcal{O}_{F1}$ ,  $\Lambda = \Lambda_1 = \Lambda_2$ .



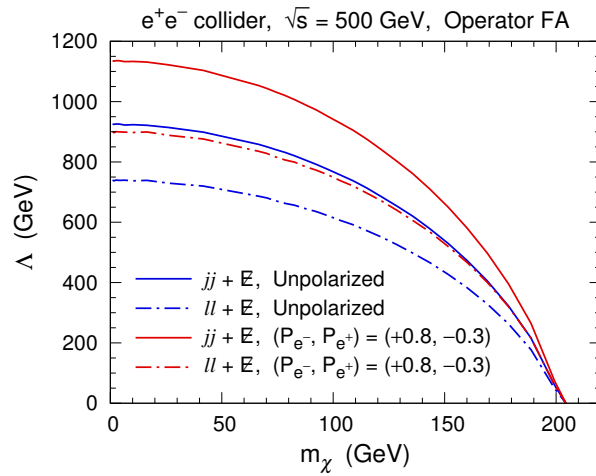
(b) 算符  $\mathcal{O}_{F2}$ ,  $\Lambda = \Lambda_1 = \Lambda_2$ .



(c) 算符  $\mathcal{O}_{FH}$ .



(d) 算符  $\mathcal{O}_{FP}$ .



(e) 算符  $\mathcal{O}_{FA}$ .

Figure 11: 非极化束流与优化的极化束流给出的  $3\sigma$  实验灵敏度曲线. 这里假设积分亮度为  $1000 \text{ fb}^{-1}$ .

## A 模型检验

**A.1 算符  $\mathcal{O}_{F1} = \frac{k_1}{\Lambda_1^3} \bar{\chi} \chi B_{\mu\nu} B^{\mu\nu} + \frac{k_2}{\Lambda_2^3} \bar{\chi} \chi W_{\mu\nu}^a W^{a\mu\nu}$**

对于指向顶点的动量  $k$ , 时空导数  $\partial_\mu$  在动量空间中贡献一个  $-ik_\mu$  因子. 利用

$$A_{\mu\nu} A^{\mu\nu} = (\partial_\mu A_\nu - \partial_\nu A_\mu)(\partial^\mu A^\nu - \partial^\nu A^\mu) = 2(\partial_\mu A_\nu \partial^\mu A^\nu - \partial_\mu A_\nu \partial^\nu A^\mu), \quad (26)$$

提取  $\chi\bar{\chi}\gamma\gamma$  顶点的 Feynman 规则:

$$\begin{aligned} \mathcal{O}_{F1} \supset G_{AA} \bar{\chi} \chi A_{\mu\nu} A^{\mu\nu} &= 2G_{AA} \bar{\chi} \chi (\partial_\mu A_\nu \partial^\mu A^\nu - \partial_\mu A_\nu \partial^\nu A^\mu) \\ &\rightarrow 2G_{AA} \bar{\chi} \chi [g^{\rho\sigma} g^{\mu\nu} \partial_\rho A_\mu(p) \partial_\sigma A_\nu(q) + g^{\rho\sigma} g^{\nu\mu} \partial_\rho A_\nu(q) \partial_\sigma A_\mu(p) \\ &\quad - g^{\rho\nu} g^{\mu\sigma} \partial_\rho A_\mu(p) \partial_\sigma A_\nu(q) - g^{\rho\mu} g^{\nu\sigma} \partial_\rho A_\nu(q) \partial_\sigma A_\mu(p)] \\ &= 4G_{AA} \bar{\chi} \chi [g^{\rho\sigma} g^{\mu\nu} \partial_\rho A_\mu(p) \partial_\sigma A_\nu(q) - g^{\rho\nu} g^{\mu\sigma} \partial_\rho A_\mu(p) \partial_\sigma A_\nu(q)] \\ &\rightarrow 4iG_{AA} [g^{\rho\sigma} g^{\mu\nu} (-ip_\rho)(-iq_\sigma) - g^{\rho\nu} g^{\mu\sigma} (-ip_\rho)(-iq_\sigma)] \\ &= -4iG_{AA} [g^{\mu\nu}(p \cdot q) - q^\mu p^\nu]. \end{aligned} \quad (27)$$

同理,  $\chi\bar{\chi}ZZ$  顶点的 Feynman 规则为

$$\begin{aligned} \mathcal{O}_{F1} \supset G_{ZZ} \bar{\chi} \chi Z_{\mu\nu} Z^{\mu\nu} &= 2G_{ZZ} \bar{\chi} \chi (\partial_\mu Z_\nu \partial^\mu Z^\nu - \partial_\mu Z_\nu \partial^\nu Z^\mu) \\ &\rightarrow 2G_{ZZ} \bar{\chi} \chi [g^{\rho\sigma} g^{\mu\nu} \partial_\rho Z_\mu(p) \partial_\sigma Z_\nu(q) + g^{\rho\sigma} g^{\nu\mu} \partial_\rho Z_\nu(q) \partial_\sigma Z_\mu(p) \\ &\quad - g^{\rho\nu} g^{\mu\sigma} \partial_\rho Z_\mu(p) \partial_\sigma Z_\nu(q) - g^{\rho\mu} g^{\nu\sigma} \partial_\rho Z_\nu(q) \partial_\sigma Z_\mu(p)] \\ &\rightarrow -4iG_{ZZ} [g^{\mu\nu}(p \cdot q) - q^\mu p^\nu], \end{aligned} \quad (28)$$

$\chi\bar{\chi}\gamma Z$  顶点的 Feynman 规则为

$$\begin{aligned} \mathcal{O}_{F1} \supset G_{AZ} \bar{\chi} \chi A_{\mu\nu} Z^{\mu\nu} &= 2G_{AZ} \bar{\chi} \chi (\partial_\mu A_\nu \partial^\mu Z^\nu - \partial_\mu A_\nu \partial^\nu Z^\mu) \\ &\rightarrow 2G_{AZ} \bar{\chi} \chi [g^{\rho\sigma} g^{\mu\nu} \partial_\rho A_\mu(p) \partial_\sigma Z_\nu(q) - g^{\rho\nu} g^{\mu\sigma} \partial_\rho A_\mu(p) \partial_\sigma Z_\nu(q)] \\ &\rightarrow 2iG_{AZ} \bar{\chi} \chi [g^{\rho\sigma} g^{\mu\nu} (-ip_\rho)(-iq_\sigma) - g^{\rho\nu} g^{\mu\sigma} (-ip_\rho)(-iq_\sigma)] \\ &= -2iG_{AZ} \bar{\chi} \chi [g^{\mu\nu}(p \cdot q) - q^\mu p^\nu]. \end{aligned} \quad (29)$$

如 Fig. 12 所示.

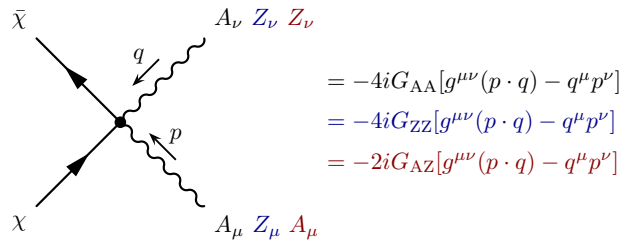


Figure 12: 算符  $\mathcal{O}_{F1}$  的 Feynman 规则.

双光子湮灭过程  $\gamma(p_1) + \gamma(p_2) \rightarrow \chi(k_1) + \bar{\chi}(k_2)$  的不变振幅为

$$i\mathcal{M} = -4iG_{AA} \bar{u}(k_1) v(k_2) [g^{\mu\nu}(p_1 \cdot p_2) - p_1^\mu p_2^\nu] \varepsilon_\mu(p_1) \varepsilon_\nu(p_2), \quad (30)$$

$$(i\mathcal{M})^* = 4iG_{AA} \bar{v}(k_2) u(k_1) [g^{\rho\sigma}(p_1 \cdot p_2) - p_2^\rho p_1^\sigma] \varepsilon_\rho^*(p_1) \varepsilon_\sigma^*(p_2). \quad (31)$$

利用

$$\text{Tr}[(\not{k}_1 + m_\chi)(\not{k}_2 - m_\chi)] = \text{Tr}(\not{k}_1 \not{k}_2 - m_\chi^2) = 4(k_1 \cdot k_2 - m_\chi^2), \quad (32)$$

$$p_1 \cdot p_2 = \frac{s}{2}, \quad k_1 \cdot k_2 = \frac{s}{2} - m_\chi^2, \quad \beta_\chi \equiv \sqrt{1 - \frac{4m_\chi^2}{s}}, \quad (33)$$

有

$$\begin{aligned}
\frac{1}{4} \sum_{\text{spins}} |\mathcal{M}|^2 &= \sum_{\text{spins}} 4G_{\text{AA}}^2 \bar{u}(k_1) v(k_2) \bar{v}(k_2) u(k_1) [g^{\mu\nu}(p_1 \cdot p_2) - p_2^\mu p_1^\nu] [g^{\rho\sigma}(p_1 \cdot p_2) - p_2^\rho p_1^\sigma] \varepsilon_\mu(p_1) \varepsilon_\rho^*(p_1) \varepsilon_\nu(p_2) \varepsilon_\sigma^*(p_2) \\
&= 4G_{\text{AA}}^2 \text{Tr}[(\not{k}_1 + m_\chi)(\not{k}_2 - m_\chi)] [g^{\mu\nu}(p_1 \cdot p_2) - p_2^\mu p_1^\nu] [g^{\rho\sigma}(p_1 \cdot p_2) - p_2^\rho p_1^\sigma] (-g_{\mu\rho})(-g_{\nu\sigma}) \\
&= 4G_{\text{AA}}^2 4(k_1 \cdot k_2 - m_\chi^2) [4(p_1 \cdot p_2)^2 - (p_1 \cdot p_2)^2 - (p_1 \cdot p_2)^2 + p_1^2 p_2^2] \\
&= 32G_{\text{AA}}^2 (k_1 \cdot k_2 - m_\chi^2) (p_1 \cdot p_2)^2 = 32G_{\text{AA}}^2 \frac{1}{2} (s - 4m_\chi^2) \frac{s^2}{4} = 4s^3 \beta_\chi^2 G_{\text{AA}}^2.
\end{aligned} \tag{34}$$

微分截面可表达成

$$\frac{d\sigma}{d\Omega} = \frac{1}{2E_{p_1} 2E_{p_2} |\mathbf{v}_1 - \mathbf{v}_2|} \frac{|\mathbf{k}_1|}{(2\pi)^2 4E_{\text{CM}}} \frac{1}{4} \sum_{\text{spins}} |\mathcal{M}|^2 = \frac{\beta_\chi}{64\pi^2 s} \frac{1}{4} \sum_{\text{spins}} |\mathcal{M}|^2, \tag{35}$$

总截面为

$$\sigma = \frac{\beta_\chi}{64\pi^2 s} \int d\Omega \frac{1}{4} \sum_{\text{spins}} |\mathcal{M}|^2 = \frac{\beta_\chi}{64\pi^2 s} 4\pi 4s^3 \beta_\chi^2 G_{\text{AA}}^2 = \frac{1}{4\pi} s^2 \beta_\chi^3 G_{\text{AA}}^2. \tag{36}$$

取

$$m_W = 80.419 \text{ GeV}, \quad m_Z = 91.188 \text{ GeV}, \quad s_W^2 = 1 - \frac{m_W^2}{m_Z^2} = 0.2222465, \quad 1 \text{ GeV}^{-2} = 3.89379304 \times 10^8 \text{ pb}, \tag{37}$$

用总截面的解析式进行计算 (记为  $\sigma$ ), 并与 MadGraph 5 计算结果 (记为  $\sigma_{\text{MG5}}$ ) 比较如下.

$$s = 1 \text{ TeV}, \quad k_1 = k_2 = 1 :$$

$$\begin{aligned}
m_\chi &= 100 \text{ GeV}, \quad \Lambda_1 = \Lambda_2 = 1 \text{ TeV}, \quad \sigma = 29.1454 \text{ pb}, \quad \sigma_{\text{MG5}} = 29.145 \text{ pb}; \\
m_\chi &= 200 \text{ GeV}, \quad \Lambda_1 = 1 \text{ TeV}, \quad \Lambda_2 \rightarrow \infty, \quad \sigma = 14.4300 \text{ pb}, \quad \sigma_{\text{MG5}} = 14.428 \text{ pb}; \\
m_\chi &= 200 \text{ GeV}, \quad \Lambda_1 \rightarrow \infty, \quad \Lambda_2 = 1 \text{ TeV}, \quad \sigma = 1.17829 \text{ pb}, \quad \sigma_{\text{MG5}} = 1.1787 \text{ pb}; \\
m_\chi &= 400 \text{ GeV}, \quad \Lambda_1 = 1 \text{ TeV}, \quad \Lambda_2 = 500 \text{ GeV}, \quad \sigma = 43.7165 \text{ pb}, \quad \sigma_{\text{MG5}} = 43.691 \text{ pb}; \\
m_\chi &= 400 \text{ GeV}, \quad \Lambda_1 = 500 \text{ GeV}, \quad \Lambda_2 = 1 \text{ TeV}, \quad \sigma = 277.949 \text{ pb}, \quad \sigma_{\text{MG5}} = 278.05 \text{ pb}.
\end{aligned}$$

$$s = 250 \text{ GeV}, \quad k_1 = k_2 = 1 :$$

$$m_\chi = 100 \text{ GeV}, \quad \Lambda_1 = \Lambda_2 = 1 \text{ TeV}, \quad \sigma = 26.1443 \text{ fb}, \quad \sigma_{\text{MG5}} = 26.157 \text{ fb}. \tag{38}$$

$Z$  玻色子湮灭过程  $Z(p_1) + Z(p_2) \rightarrow \chi(k_1) + \bar{\chi}(k_2)$  的不变振幅为

$$i\mathcal{M} = -4iG_{\text{ZZ}} \bar{u}(k_1) v(k_2) [g^{\mu\nu}(p_1 \cdot p_2) - p_2^\mu p_1^\nu] \varepsilon_\mu(p_1) \varepsilon_\nu(p_2), \tag{39}$$

$$(i\mathcal{M})^* = 4iG_{\text{ZZ}} \bar{v}(k_2) u(k_1) [g^{\rho\sigma}(p_1 \cdot p_2) - p_2^\rho p_1^\sigma] \varepsilon_\rho^*(p_1) \varepsilon_\sigma^*(p_2). \tag{40}$$

利用 (32) 式和

$$p_1 \cdot p_2 = \frac{s}{2} - m_Z^2, \quad k_1 \cdot k_2 = \frac{s}{2} - m_\chi^2, \quad \beta_Z \equiv \sqrt{1 - \frac{4m_Z^2}{s}}, \quad \beta_\chi \equiv \sqrt{1 - \frac{4m_\chi^2}{s}}, \tag{41}$$

以及  $Z$  玻色子极化矢量求和关系

$$\sum_{\text{spins}} \varepsilon_\mu(p) \varepsilon_\nu^*(p) = -g_{\mu\nu} + \frac{p_\mu p_\nu}{m_Z^2}, \tag{42}$$

有

$$\begin{aligned}
&\frac{1}{9} \sum_{\text{spins}} |\mathcal{M}|^2 \\
&= \sum_{\text{spins}} \frac{16}{9} G_{\text{ZZ}}^2 \bar{u}(k_1) v(k_2) \bar{v}(k_2) u(k_1) [g^{\mu\nu}(p_1 \cdot p_2) - p_2^\mu p_1^\nu] [g^{\rho\sigma}(p_1 \cdot p_2) - p_2^\rho p_1^\sigma] \varepsilon_\mu(p_1) \varepsilon_\rho^*(p_1) \varepsilon_\nu(p_2) \varepsilon_\sigma^*(p_2)
\end{aligned}$$

$$\begin{aligned}
&= \frac{16}{9} G_{ZZ}^2 \text{Tr}[(\not{k}_1 + m_\chi)(\not{k}_2 - m_\chi)][g^{\mu\nu}(p_1 \cdot p_2) - p_2^\mu p_1^\nu] \left( -g_{\mu\rho} + \frac{p_{1\mu} p_{1\rho}}{m_Z^2} \right) [g^{\rho\sigma}(p_1 \cdot p_2) - p_2^\rho p_1^\sigma] \left( -g_{\nu\sigma} + \frac{p_{2\nu} p_{2\sigma}}{m_Z^2} \right) \\
&= \frac{16}{9} G_{ZZ}^2 4(k_1 \cdot k_2 - m_\chi^2) [-\delta^\nu_\rho (p_1 \cdot p_2) + p_1^\nu p_{2\rho}] [-\delta^\rho_\nu (p_1 \cdot p_2) + p_{1\nu} p_2^\rho] \\
&= \frac{64}{9} G_{ZZ}^2 (k_1 \cdot k_2 - m_\chi^2) [2(p_1 \cdot p_2)^2 + m_Z^4] = \frac{64}{9} G_{ZZ}^2 \frac{1}{2} (s - 4m_\chi^2) \frac{1}{2} (s^2 - 4sm_Z^2 + 6m_Z^4) \\
&= \frac{16}{9} s \beta_\chi^2 (s^2 \beta_Z^2 + 6m_Z^4) G_{ZZ}^2.
\end{aligned} \tag{43}$$

微分截面可表达成

$$\frac{d\sigma}{d\Omega} = \frac{1}{2E_{p_1} 2E_{p_2} |\mathbf{v}_1 - \mathbf{v}_2|} \frac{|\mathbf{k}_1|}{(2\pi)^2 4E_{\text{CM}}} \frac{1}{9} \sum_{\text{spins}} |\mathcal{M}|^2 = \frac{\beta_\chi}{64\pi^2 s \beta_Z} \frac{1}{9} \sum_{\text{spins}} |\mathcal{M}|^2, \tag{44}$$

总截面为

$$\sigma = \frac{\beta_\chi}{64\pi^2 s \beta_Z} \int d\Omega \frac{1}{9} \sum_{\text{spins}} |\mathcal{M}|^2 = \frac{\beta_\chi}{64\pi^2 s \beta_Z} 4\pi \frac{16}{9} s \beta_\chi^2 (s^2 \beta_Z^2 + 6m_Z^4) G_{ZZ}^2 = \frac{s^2 \beta_\chi^3 G_{ZZ}^2}{9\pi} \left( \beta_Z + \frac{6m_Z^4}{s^2 \beta_Z} \right). \tag{45}$$

解析计算与 MadGraph 5 计算结果比较如下.

$$\begin{aligned}
s = 1 \text{ TeV}, \quad k_1 = k_2 = 1 : \\
m_\chi = 100 \text{ GeV}, \quad \Lambda_1 = \Lambda_2 = 1 \text{ TeV}, \quad \sigma = 12.7417 \text{ pb}, \quad \sigma_{\text{MG5}} = 12.742 \text{ pb}; \\
m_\chi = 200 \text{ GeV}, \quad \Lambda_1 = 1 \text{ TeV}, \quad \Lambda_2 \rightarrow \infty, \quad \sigma = 0.515122 \text{ pb}, \quad \sigma_{\text{MG5}} = 0.51514 \text{ pb}; \\
m_\chi = 200 \text{ GeV}, \quad \Lambda_1 \rightarrow \infty, \quad \Lambda_2 = 1 \text{ TeV}, \quad \sigma = 6.30847 \text{ pb}, \quad \sigma_{\text{MG5}} = 6.3056 \text{ pb}; \\
m_\chi = 400 \text{ GeV}, \quad \Lambda_1 = 1 \text{ TeV}, \quad \Lambda_2 = 500 \text{ GeV}, \quad \sigma = 121.513 \text{ pb}, \quad \sigma_{\text{MG5}} = 121.49 \text{ pb}; \\
m_\chi = 400 \text{ GeV}, \quad \Lambda_1 = 500 \text{ GeV}, \quad \Lambda_2 = 1 \text{ TeV}, \quad \sigma = 19.1119 \text{ pb}, \quad \sigma_{\text{MG5}} = 19.101 \text{ pb}. \\
s = 250 \text{ GeV}, \quad k_1 = k_2 = 1 : \\
m_\chi = 100 \text{ GeV}, \quad \Lambda_1 = \Lambda_2 = 1 \text{ TeV}, \quad \sigma = 9.75183 \text{ fb}, \quad \sigma_{\text{MG5}} = 9.7555 \text{ fb}.
\end{aligned} \tag{46}$$

对于算符  $\mathcal{O}_{F1}$ , 暗物质湮灭过程  $\chi\bar{\chi} \rightarrow ZZ$  是  $p$  波压低的.

**A.2 算符  $\mathcal{O}_{F2} = \frac{k_1}{\Lambda_1^3} \bar{\chi} i \gamma_5 \chi B_{\mu\nu} \tilde{B}^{\mu\nu} + \frac{k_2}{\Lambda_2^3} \bar{\chi} i \gamma_5 \chi W_{\mu\nu}^a \tilde{W}^{a\mu\nu}$**

利用

$$Z_{\mu\nu} \tilde{Z}^{\mu\nu} \equiv \frac{1}{2} \varepsilon^{\mu\nu\rho\sigma} Z_{\mu\nu} Z_{\rho\sigma} = \frac{1}{2} \varepsilon^{\mu\nu\rho\sigma} (\partial_\mu Z_\nu - \partial_\nu Z_\mu) (\partial_\rho Z_\sigma - \partial_\sigma Z_\rho) = 2\varepsilon^{\mu\nu\rho\sigma} \partial_\mu Z_\nu \partial_\rho Z_\sigma, \tag{47}$$

提取  $\chi\bar{\chi}ZZ$  顶点的 Feynman 规则:

$$\begin{aligned}
\mathcal{O}_{F2} \supset G_{ZZ} \bar{\chi} i \gamma_5 \chi Z_{\mu\nu} \tilde{Z}^{\mu\nu} &= 2G_{ZZ} \bar{\chi} i \gamma_5 \chi \varepsilon^{\rho\mu\sigma\nu} \partial_\rho Z_\mu \partial_\sigma Z_\nu \\
&\rightarrow 2G_{ZZ} \bar{\chi} i \gamma_5 \chi [\varepsilon^{\rho\mu\sigma\nu} \partial_\rho Z_\mu(p) \partial_\sigma Z_\nu(q) + \varepsilon^{\rho\nu\sigma\mu} \partial_\rho Z_\nu(q) \partial_\sigma Z_\mu(p)] \\
&\rightarrow -2G_{ZZ} \gamma_5 [\varepsilon^{\rho\mu\sigma\nu} (-ip_\rho) (-iq_\sigma) + \varepsilon^{\rho\nu\sigma\mu} (-iq_\rho) (-ip_\sigma)] \\
&= -4G_{ZZ} \gamma_5 \varepsilon^{\mu\nu\rho\sigma} p_\rho q_\sigma.
\end{aligned} \tag{48}$$

同理,  $\chi\bar{\chi}Z$  顶点的 Feynman 规则为

$$\begin{aligned}
\mathcal{O}_{F2} \supset G_{AZ} \bar{\chi} i \gamma_5 \chi A_{\mu\nu} \tilde{Z}^{\mu\nu} &= 2G_{AZ} \bar{\chi} i \gamma_5 \chi \varepsilon^{\rho\mu\sigma\nu} \partial_\rho A_\mu \partial_\sigma Z_\nu \\
&\rightarrow 2G_{AZ} \bar{\chi} i \gamma_5 \chi \varepsilon^{\rho\mu\sigma\nu} \partial_\rho A_\mu(p) \partial_\sigma Z_\nu(q) \\
&\rightarrow -2G_{AZ} \gamma_5 \varepsilon^{\rho\mu\sigma\nu} (-ip_\rho) (-iq_\sigma) \\
&= -2G_{AZ} \gamma_5 \varepsilon^{\mu\nu\rho\sigma} p_\rho q_\sigma.
\end{aligned} \tag{49}$$

如 Fig. 13 所示.

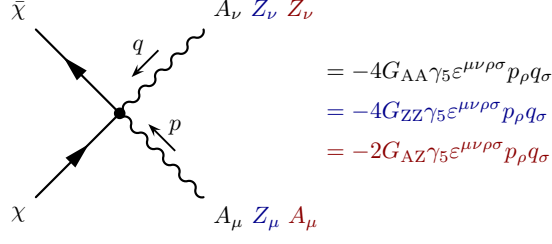


Figure 13: 算符  $\mathcal{O}_{F2}$  的 Feynman 规则.

$Z$  玻色子湮灭过程  $Z(p_1) + Z(p_2) \rightarrow \chi(k_1) + \bar{\chi}(k_2)$  的不变振幅为

$$i\mathcal{M} = -4G_{ZZ}\bar{u}(k_1)\gamma_5 v(k_2)\varepsilon^{\mu\nu\rho\sigma}p_{1\rho}p_{2\sigma}\varepsilon_\mu(p_1)\varepsilon_\nu(p_2), \quad (50)$$

$$(i\mathcal{M})^* = 4G_{ZZ}\bar{v}(k_2)\gamma_5 u(k_1)\varepsilon^{\alpha\beta\gamma\delta}p_{1\gamma}p_{2\delta}\varepsilon_\alpha^*(p_1)\varepsilon_\beta^*(p_2). \quad (51)$$

利用 (41) 式和

$$\text{Tr}[(\not{k}_1 + m_\chi)\gamma_5(\not{k}_2 - m_\chi)\gamma_5] = \text{Tr}(-\not{k}_1\not{k}_2 - m_\chi^2) = -4(k_1 \cdot k_2 + m_\chi^2), \quad (52)$$

$$\varepsilon^{\mu\nu\rho\sigma}\varepsilon_{\mu\nu\gamma\delta} = -2!2!\delta^{[\rho}_\gamma\delta^{\sigma]}_\delta = 2(\delta^\sigma_\gamma\delta^\rho_\delta - \delta^\rho_\gamma\delta^\sigma_\delta), \quad (53)$$

$$\varepsilon^{\mu\nu\rho\sigma}\varepsilon_{\mu\nu\gamma\delta}p_{1\rho}p_{2\sigma}p_1^\gamma p_2^\delta = 2(\delta^\sigma_\gamma\delta^\rho_\delta p_{1\rho}p_{2\sigma}p_1^\gamma p_2^\delta - \delta^\rho_\gamma\delta^\sigma_\delta p_{1\rho}p_{2\sigma}p_1^\gamma p_2^\delta) = 2[(p_1 \cdot p_2)^2 - m_Z^4], \quad (54)$$

有

$$\begin{aligned} & \frac{1}{9} \sum_{\text{spins}} |\mathcal{M}|^2 \\ &= - \sum_{\text{spins}} \frac{16}{9} G_{ZZ}^2 \bar{u}(k_1)\gamma_5 v(k_2)\bar{v}(k_2)\gamma_5 u(k_1)\varepsilon^{\mu\nu\rho\sigma}\varepsilon^{\alpha\beta\gamma\delta}p_{1\rho}p_{2\sigma}p_{1\gamma}p_{2\delta}\varepsilon_\mu(p_1)\varepsilon_\alpha^*(p_1)\varepsilon_\nu(p_2)\varepsilon_\beta^*(p_2) \\ &= -\frac{16}{9} G_{ZZ}^2 \text{Tr}[(\not{k}_1 + m_\chi)\gamma_5(\not{k}_2 - m_\chi)\gamma_5]\varepsilon^{\mu\nu\rho\sigma}p_{1\rho}p_{2\sigma} \left( -g_{\mu\alpha} + \frac{p_{1\mu}p_{1\alpha}}{m_Z^2} \right) \varepsilon^{\alpha\beta\gamma\delta}p_{1\gamma}p_{2\delta} \left( -g_{\nu\beta} + \frac{p_{2\nu}p_{2\beta}}{m_Z^2} \right) \\ &= \frac{64}{9} G_{ZZ}^2 (k_1 \cdot k_2 + m_\chi^2) \varepsilon^{\mu\nu\rho\sigma}\varepsilon_{\mu\nu\gamma\delta}p_{1\rho}p_{2\sigma}p_1^\gamma p_2^\delta = \frac{128}{9} G_{ZZ}^2 (k_1 \cdot k_2 + m_\chi^2) [(p_1 \cdot p_2)^2 - m_Z^4] \\ &= \frac{128}{9} G_{ZZ}^2 \frac{s}{2} \frac{1}{4} [(s - 2m_Z^2)^2 - 4m_Z^4] = \frac{16}{9} G_{ZZ}^2 s(s^2 - 4sm_Z^2) = \frac{16}{9} s^3 \beta_Z^2 G_{ZZ}^2. \end{aligned} \quad (55)$$

总截面为

$$\sigma = \frac{\beta_\chi}{64\pi^2 s \beta_Z} \int d\Omega \frac{1}{9} \sum_{\text{spins}} |\mathcal{M}|^2 = \frac{\beta_\chi}{64\pi^2 s \beta_Z} 4\pi \frac{16}{9} s^3 \beta_Z^2 G_{ZZ}^2 = \frac{1}{9\pi} s^2 \beta_\chi \beta_Z G_{ZZ}^2. \quad (56)$$

解析计算与 MadGraph 5 计算结果比较如下.

$$\begin{aligned} & s = 1 \text{ TeV}, \quad k_1 = k_2 = 1 : \\ & \quad m_\chi = 100 \text{ GeV}, \quad \Lambda_1 = \Lambda_2 = 1 \text{ TeV}, \quad \sigma = 13.2669 \text{ pb}, \quad \sigma_{\text{MG5}} = 13.267 \text{ pb}. \\ & s = 250 \text{ GeV}, \quad k_1 = k_2 = 1 : \\ & \quad m_\chi = 100 \text{ GeV}, \quad \Lambda_1 = \Lambda_2 = 1 \text{ TeV}, \quad \sigma = 22.0766 \text{ fb}, \quad \sigma_{\text{MG5}} = 22.077 \text{ fb}. \end{aligned} \quad (57)$$

对于暗物质湮灭过程  $\chi(p_1) + \bar{\chi}(p_2) \rightarrow Z(k_1) + Z(k_2)$ , 不变振幅为

$$\begin{aligned} i\mathcal{M} &= -4G_{ZZ}\bar{v}(p_2)\gamma_5 u(p_1)\varepsilon^{\mu\nu\rho\sigma}(-k_{1\rho})(-k_{2\sigma})\varepsilon_\mu(k_1)\varepsilon_\nu(k_2), \\ (i\mathcal{M})^* &= 4G_{ZZ}\bar{u}(p_1)\gamma_5 v(p_2)\varepsilon^{\alpha\beta\gamma\delta}(-k_{1\gamma})(-k_{2\delta})\varepsilon_\alpha^*(k_1)\varepsilon_\beta^*(k_2). \end{aligned} \quad (58)$$

利用 (53) 式及

$$\text{Tr}[(\not{p}_2 - m_\chi)\gamma_5(\not{p}_1 + m_\chi)\gamma_5] = \text{Tr}(-\not{p}_2\not{p}_1 - m_\chi^2) = -4(p_1 \cdot p_2 + m_\chi^2),$$

$$p_1 \cdot p_2 = \frac{s}{2} - m_\chi^2, \quad k_1 \cdot k_2 = \frac{s}{2} - m_Z^2, \quad (59)$$

有

$$\begin{aligned} \frac{1}{4} \sum_{\text{spins}} |\mathcal{M}|^2 &= - \sum_{\text{spins}} 4G_{ZZ}^2 \bar{v}(p_2) \gamma_5 u(p_1) \bar{u}(p_1) \gamma_5 v(p_2) \varepsilon^{\mu\nu\rho\sigma} k_{1\rho} k_{2\sigma} \varepsilon^{\alpha\beta\gamma\delta} k_{1\gamma} k_{2\delta} \varepsilon_\mu(k_1) \varepsilon_\alpha^*(k_1) \varepsilon_\nu(k_2) \varepsilon_\beta^*(k_2) \\ &= -4G_{ZZ}^2 \text{Tr}[(\not{p}_2 - m_\chi) \gamma_5 (\not{p}_1 + m_\chi) \gamma_5] \varepsilon^{\mu\nu\rho\sigma} k_{1\rho} k_{2\sigma} \left( -g_{\mu\alpha} + \frac{k_{1\mu} k_{1\alpha}}{m_Z^2} \right) \varepsilon^{\alpha\beta\gamma\delta} k_{1\gamma} k_{2\delta} \left( -g_{\nu\beta} + \frac{k_{2\nu} k_{2\beta}}{m_Z^2} \right) \\ &= 16G_{ZZ}^2 (p_1 \cdot p_2 + m_\chi^2) \varepsilon^{\mu\nu\rho\sigma} \varepsilon_{\mu\nu}{}^{\gamma\delta} k_{1\rho} k_{2\sigma} k_{1\gamma} k_{2\delta} = 16G_{ZZ}^2 (p_1 \cdot p_2 + m_\chi^2) 2[(k_1 \cdot k_2)^2 - m_Z^4] \\ &= 32G_{ZZ}^2 \frac{s}{2} \frac{1}{4} (s^2 - 4sm_Z^2) = 4s^3 \beta_Z^2 G_{ZZ}^2. \end{aligned} \quad (60)$$

微分截面可表达成

$$\frac{d\sigma}{d\Omega} = \frac{1}{2E_{p_1} 2E_{p_2} |\mathbf{v}_1 - \mathbf{v}_2|} \frac{|\mathbf{k}_1|}{(2\pi)^2 4E_{\text{CM}}} \frac{1}{4} \sum_{\text{spins}} |\mathcal{M}|^2 = \frac{\beta_Z}{64\pi^2 s \beta_\chi} \frac{1}{4} \sum_{\text{spins}} |\mathcal{M}|^2, \quad (61)$$

注意到末态粒子全同性, 总截面为

$$\sigma = \frac{\beta_Z}{64\pi^2 s \beta_\chi} \frac{1}{2} \int d\Omega \frac{1}{4} \sum_{\text{spins}} |\mathcal{M}|^2 = \frac{\beta_Z}{64\pi^2 s \beta_\chi} \frac{1}{2} 4\pi 4s^3 \beta_Z^2 G_{ZZ}^2 = \frac{s^2 G_{ZZ}^2 \beta_Z^3}{8\pi \beta_\chi}. \quad (62)$$

在质心系中, 暗物质粒子之间的相对速度  $v_{\text{rel}} = |\mathbf{v}_1 - \mathbf{v}_2| = 2\beta_\chi$ . 在低速近似下,  $s \simeq 4m_\chi^2$ ,  $\beta_Z \simeq \sqrt{1 - \frac{m_Z^2}{m_\chi^2}}$ , 则

$$\langle \sigma v_{\text{rel}} \rangle = 2\beta_\chi \sigma = \frac{s^2 G_{ZZ}^2 \beta_Z^3}{4\pi} \simeq \frac{4m_\chi^4 G_{ZZ}^2 \beta_Z^3}{\pi}. \quad (63)$$

当  $k_1 = k_2 = 1$ ,  $m_\chi = 150$  GeV,  $\Lambda_1 = \Lambda_2 = 1$  TeV 时, 对于  $\sqrt{s} = 500$  GeV, 解析计算与 MadGraph 5 计算的结果分别为  $\sigma = 977.054$  fb 和  $\sigma_{\text{MG5}} = 977.00$  fb. 利用

$$1 \text{ GeV}^{-2} = 1.1673297854 \times 10^{-17} \text{ cm}^3 \text{ s}^{-1}, \quad (64)$$

对于  $s \simeq 4m_\chi^2$ ,  $\langle \sigma v_{\text{rel}} \rangle = 3.7664 \times 10^{-27} \text{ cm}^3 \text{ s}^{-1}$ .

### A.3 算符 $\mathcal{O}_{\text{FH}} = \frac{1}{\Lambda^3} \bar{\chi} \chi (D_\mu H)^\dagger D_\mu H$

$\chi \bar{\chi} Z Z$  顶点的 Feynman 规则为

$$\begin{aligned} \mathcal{O}_{\text{FH}} &\supset \frac{m_Z^2}{2\Lambda^3} \bar{\chi} \chi Z_\mu Z^\mu \\ &\rightarrow \frac{m_Z^2}{2\Lambda^3} \bar{\chi} \chi [g^{\mu\nu} Z_\mu(p) Z_\nu(q) + g^{\nu\mu} Z_\nu(q) Z_\mu(p)] = \frac{m_Z^2}{\Lambda^3} \bar{\chi} \chi g^{\mu\nu} Z_\mu(p) Z_\nu(q) \\ &\rightarrow i \frac{m_Z^2}{\Lambda^3} g^{\mu\nu}. \end{aligned} \quad (65)$$

如 Fig. 14 所示.

$Z$  玻色子湮灭过程  $Z(p_1) + Z(p_2) \rightarrow \chi(k_1) + \bar{\chi}(k_2)$  的不变振幅为

$$i\mathcal{M} = i \frac{m_Z^2}{\Lambda^3} \bar{u}(k_1) v(k_2) g^{\mu\nu} \varepsilon_\mu(p_1) \varepsilon_\nu(p_2), \quad (66)$$

$$(i\mathcal{M})^* = -i \frac{m_Z^2}{\Lambda^3} \bar{v}(k_2) u(k_1) g^{\rho\sigma} \varepsilon_\rho^*(p_1) \varepsilon_\sigma^*(p_2). \quad (67)$$

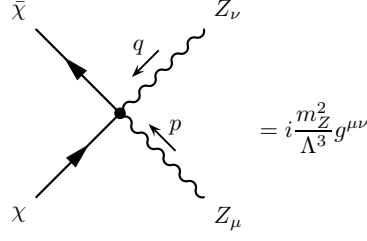


Figure 14: 对于算符  $\mathcal{O}_{\text{FH}}$ ,  $\chi\bar{\chi}ZZ$  顶点的 Feynman 规则.

利用 (32) 和 (41) 式, 有

$$\begin{aligned}
\frac{1}{9} \sum_{\text{spins}} |\mathcal{M}|^2 &= \frac{1}{9} \sum_{\text{spins}} \frac{m_Z^4}{\Lambda^6} \bar{u}(k_1) v(k_2) \bar{v}(k_2) u(k_1) g^{\mu\nu} g^{\rho\sigma} \varepsilon_\mu(p_1) \varepsilon_\rho^*(p_1) \varepsilon_\nu(p_2) \varepsilon_\sigma^*(p_2) \\
&= \frac{m_Z^4}{9\Lambda^6} \text{Tr}[(\not{k}_1 + m_\chi)(\not{k}_2 - m_\chi)] g^{\mu\nu} g^{\rho\sigma} \left( -g_{\mu\rho} + \frac{p_{1\mu} p_{1\rho}}{m_Z^2} \right) \left( -g_{\nu\sigma} + \frac{p_{2\nu} p_{2\sigma}}{m_Z^2} \right) \\
&= \frac{m_Z^4}{9\Lambda^6} 4(k_1 \cdot k_2 - m_\chi^2) \left( \delta^\nu_\rho - \frac{p_1^\nu p_{1\rho}}{m_Z^2} \right) \left( \delta^\rho_\nu - \frac{p_2^\rho p_{2\nu}}{m_Z^2} \right) = \frac{m_Z^4}{9\Lambda^6} 4(k_1 \cdot k_2 - m_\chi^2) \left[ 2 + \frac{(p_1 \cdot p_2)^2}{m_Z^4} \right] \\
&= \frac{4m_Z^4}{9\Lambda^6} \frac{1}{2} (s - 4m_\chi^2) \left[ 2 + \frac{1}{4m_Z^4} (s - 2m_Z^2)^2 \right] = \frac{2m_Z^4 s \beta_\chi^2}{9\Lambda^6} \left( 3 + \frac{s^2 \beta_Z^2}{4m_Z^4} \right). \tag{68}
\end{aligned}$$

总截面为

$$\sigma = \frac{\beta_\chi}{64\pi^2 s \beta_Z} \int d\Omega \frac{1}{9} \sum_{\text{spins}} |\mathcal{M}|^2 = \frac{\beta_\chi}{64\pi^2 s \beta_Z} 4\pi \frac{2m_Z^4 s \beta_\chi^2}{9\Lambda^6} \left( 3 + \frac{s^2 \beta_Z^2}{4m_Z^4} \right) = \frac{m_Z^4 \beta_\chi^3}{72\pi \Lambda^6 \beta_Z} \left( 3 + \frac{s^2 \beta_Z^2}{4m_Z^4} \right). \tag{69}$$

解析计算与 MadGraph 5 计算结果比较如下.

$$\begin{aligned}
s &= 1 \text{ TeV}, \quad m_\chi = 100 \text{ GeV}, \quad \Lambda = 1 \text{ TeV}, \quad \sigma = 0.398350 \text{ pb}, \quad \sigma_{\text{MG5}} = 0.39834 \text{ pb}; \\
s &= 250 \text{ GeV}, \quad m_\chi = 100 \text{ GeV}, \quad \Lambda = 1 \text{ TeV}, \quad \sigma = 0.361127 \text{ fb}, \quad \sigma_{\text{MG5}} = 0.36123 \text{ fb}.
\end{aligned} \tag{70}$$

对于算符  $\mathcal{O}_{\text{FH}}$ , 暗物质湮灭过程  $\chi\bar{\chi} \rightarrow ZZ$  是  $p$  波压低的.

#### A.4 算符 $\mathcal{O}_{\text{FP}} = \frac{1}{\Lambda^2} \bar{\chi} \gamma_5 \chi \bar{e} \gamma_5 e$

正负电子湮灭过程  $e^-(p_1) + e^+(p_2) \rightarrow \chi(k_1) + \bar{\chi}(k_2)$  的不变振幅为

$$\begin{aligned}
i\mathcal{M} &= \frac{i}{\Lambda^2} \bar{v}(p_2) \gamma_5 u(p_1) \bar{u}(k_1) \gamma_5 v(k_2), \\
(i\mathcal{M})^* &= -\frac{i}{\Lambda^2} \bar{u}(p_1) \gamma_5 v(p_2) \bar{v}(k_2) \gamma_5 u(k_1).
\end{aligned} \tag{71}$$

利用 (52) 式和

$$\text{Tr}[(\not{p}_2 - m_e) \gamma_5 (\not{p}_1 + m_e) \gamma_5] = \text{Tr}(-\not{p}_2 \not{p}_1 - m_e^2) = -4(p_1 \cdot p_2 + m_e^2), \tag{72}$$

$$p_1 \cdot p_2 = \frac{s}{2} - m_e^2, \quad k_1 \cdot k_2 = \frac{s}{2} - m_\chi^2, \quad \beta_e \equiv \sqrt{1 - \frac{4m_e^2}{s}}, \quad \beta_\chi \equiv \sqrt{1 - \frac{4m_\chi^2}{s}}, \tag{73}$$

有

$$\begin{aligned}
\frac{1}{4} \sum_{\text{spins}} |\mathcal{M}|^2 &= \sum_{\text{spins}} \frac{1}{4\Lambda^4} \bar{v}(p_2) \gamma_5 u(p_1) \bar{u}(p_1) \gamma_5 v(p_2) \bar{u}(k_1) \gamma_5 v(k_2) \bar{v}(k_2) \gamma_5 u(k_1) \\
&= \frac{1}{4\Lambda^4} \text{Tr}[(\not{p}_2 - m_e) \gamma_5 (\not{p}_1 + m_e) \gamma_5] \text{Tr}[(\not{k}_1 + m_\chi) \gamma_5 (\not{k}_2 - m_\chi) \gamma_5]
\end{aligned}$$



$$= \frac{4}{\Lambda^4} (p_1 \cdot p_2 + m_e^2) (k_1 \cdot k_2 + m_\chi^2) = \frac{s^2}{\Lambda^4}. \quad (74)$$

微分截面可表达成

$$\frac{d\sigma}{d\Omega} = \frac{1}{2E_{p_1} 2E_{p_2} |\mathbf{v}_1 - \mathbf{v}_2|} \frac{|\mathbf{k}_1|}{(2\pi)^2 4E_{\text{CM}}} \frac{1}{4} \sum_{\text{spins}} |\mathcal{M}|^2 = \frac{\beta_\chi}{64\pi^2 s \beta_e} \frac{1}{4} \sum_{\text{spins}} |\mathcal{M}|^2, \quad (75)$$

总截面为

$$\sigma = \frac{\beta_\chi}{64\pi^2 s \beta_e} \int d\Omega \frac{1}{4} \sum_{\text{spins}} |\mathcal{M}|^2 = \frac{\beta_\chi}{64\pi^2 s \beta_e} 4\pi \frac{s^2}{\Lambda^4} = \frac{s \beta_\chi}{16\pi \Lambda^4 \beta_e}. \quad (76)$$

解析计算与 MadGraph 5 计算结果比较如下.

$$s = 250 \text{ GeV}, \quad m_\chi = 100 \text{ GeV}, \quad \Lambda = 1 \text{ TeV}, \quad \sigma = 0.290492 \text{ fb}, \quad \sigma_{\text{MG5}} = 0.29057 \text{ fb}. \quad (77)$$

暗物质湮灭过程  $\chi(p_1) + \bar{\chi}(p_2) \rightarrow e^-(k_1) + e^+(k_2)$  与  $e^-(p_1) + e^+(p_2) \rightarrow \chi(k_1) + \bar{\chi}(k_2)$  类似, 只需作替换  $m_\chi \leftrightarrow m_e$ , 就可以套用它的结果. 因此,

$$\frac{1}{4} \sum_{\text{spins}} |\mathcal{M}|^2 = \frac{4}{\Lambda^4} (p_1 \cdot p_2 + m_\chi^2) (k_1 \cdot k_2 + m_e^2) = \frac{s^2}{\Lambda^4}. \quad (78)$$

微分截面可表达成

$$\frac{d\sigma}{d\Omega} = \frac{1}{2E_{p_1} 2E_{p_2} |\mathbf{v}_1 - \mathbf{v}_2|} \frac{|\mathbf{k}_1|}{(2\pi)^2 4E_{\text{CM}}} \frac{1}{4} \sum_{\text{spins}} |\mathcal{M}|^2 = \frac{\beta_e}{64\pi^2 s \beta_\chi} \frac{1}{4} \sum_{\text{spins}} |\mathcal{M}|^2, \quad (79)$$

总截面为

$$\sigma = \frac{\beta_e}{64\pi^2 s \beta_\chi} \int d\Omega \frac{1}{4} \sum_{\text{spins}} |\mathcal{M}|^2 = \frac{\beta_e}{64\pi^2 s \beta_\chi} 4\pi \frac{s^2}{\Lambda^4} = \frac{s \beta_e}{16\pi \Lambda^4 \beta_\chi}. \quad (80)$$

在低速近似下,  $\beta_e \simeq \sqrt{1 - \frac{m_e^2}{m_\chi^2}}$ ,

$$\langle \sigma v_{\text{rel}} \rangle = 2\beta_\chi \sigma = \frac{s \beta_e}{8\pi \Lambda^4} \simeq \frac{m_\chi^2 \beta_e}{2\pi \Lambda^4}. \quad (81)$$

当  $k_1 = k_2 = 1$ ,  $m_\chi = 150 \text{ GeV}$ ,  $\Lambda_1 = \Lambda_2 = 1 \text{ TeV}$  时, 对于  $\sqrt{s} = 500 \text{ GeV}$ , 解析计算与 MadGraph 5 计算的结果分别为  $\sigma = 2.42077 \text{ pb}$  和  $\sigma_{\text{MG5}} = 2.4206 \text{ pb}$ . 对于  $s \simeq 4m_\chi^2$ ,  $\langle \sigma v_{\text{rel}} \rangle = 4.1802 \times 10^{-26} \text{ cm}^3 \text{ s}^{-1}$ .

## A.5 算符 $\mathcal{O}_{\text{FA}} = \frac{1}{\Lambda^2} \bar{\chi} \gamma^\mu \gamma_5 \chi \bar{e} \gamma_\mu \gamma_5 e$

正负电子湮灭过程  $e^-(p_1) + e^+(p_2) \rightarrow \chi(k_1) + \bar{\chi}(k_2)$  的不变振幅为

$$\begin{aligned} i\mathcal{M} &= \frac{i}{\Lambda^2} \bar{v}(p_2) \gamma^\mu \gamma_5 u(p_1) \bar{u}(k_1) \gamma_\mu \gamma_5 v(k_2), \\ (i\mathcal{M})^* &= -\frac{i}{\Lambda^2} \bar{u}(p_1) \gamma^\nu \gamma_5 v(p_2) \bar{v}(k_2) \gamma_\nu \gamma_5 u(k_1). \end{aligned} \quad (82)$$

利用 (73) 式和

$$\begin{aligned} \text{Tr}(\gamma^\rho \gamma^\mu \gamma^\sigma \gamma^\nu) &= 4(g^{\rho\mu} g^{\sigma\nu} - g^{\rho\sigma} g^{\mu\nu} + g^{\rho\nu} g^{\mu\sigma}), \quad \text{Tr}(\gamma^\mu \gamma^\nu) = 4g^{\mu\nu}, \\ \text{Tr}(\not{p}_2 \gamma^\mu \not{p}_1 \gamma^\nu) &= 4(g^{\rho\mu} g^{\sigma\nu} - g^{\rho\sigma} g^{\mu\nu} + g^{\rho\nu} g^{\mu\sigma}) p_{2\rho} p_{1\sigma} = 4[p_2^\mu p_1^\nu - g^{\mu\nu} (p_1 \cdot p_2) + p_2^\nu p_1^\mu], \\ \text{Tr}[(\not{p}_2 - m_e) \gamma^\mu \gamma_5 (\not{p}_1 + m_e) \gamma^\nu \gamma_5] &= \text{Tr}(\not{p}_2 \gamma^\mu \not{p}_1 \gamma^\nu + m_e^2 \gamma^\mu \gamma^\nu) = 4[p_2^\mu p_1^\nu - g^{\mu\nu} (p_1 \cdot p_2) + p_2^\nu p_1^\mu + g^{\mu\nu} m_e^2], \\ \text{Tr}[(\not{k}_1 + m_\chi) \gamma_\mu \gamma_5 (\not{k}_2 - m_\chi) \gamma_\nu \gamma_5] &= \text{Tr}(\not{k}_1 \gamma_\mu \not{k}_2 \gamma_\nu + m_\chi^2 \gamma_\mu \gamma_\nu) = 4[k_{1\mu} k_{2\nu} - g_{\mu\nu} (k_1 \cdot k_2) + k_{1\nu} k_{2\mu} + g_{\mu\nu} m_\chi^2], \\ p_1 \cdot k_1 &= \frac{\sqrt{s}}{2} \frac{\sqrt{s}}{2} - |\mathbf{p}_1| |\mathbf{k}_1| \cos \theta = \frac{s}{4} (1 - \beta_e \beta_\chi \cos \theta) = p_2 \cdot k_2, \end{aligned} \quad (83)$$

$$p_1 \cdot k_2 = \frac{\sqrt{s}}{2} \frac{\sqrt{s}}{2} - |\mathbf{p}_1| |\mathbf{k}_2| \cos(\pi - \theta) = \frac{s}{4} (1 + \beta_e \beta_\chi \cos \theta) = p_2 \cdot k_1, \quad (85)$$

有

$$\begin{aligned} \frac{1}{4} \sum_{\text{spins}} |\mathcal{M}|^2 &= \sum_{\text{spins}} \frac{1}{4\Lambda^4} \bar{v}(p_2) \gamma^\mu \gamma_5 u(p_1) \bar{u}(p_1) \gamma^\nu \gamma_5 v(p_2) \bar{u}(k_1) \gamma_\mu \gamma_5 v(k_2) \bar{v}(k_2) \gamma_\nu \gamma_5 u(k_1) \\ &= \frac{1}{4\Lambda^4} \text{Tr}[(\not{p}_2 - m_e) \gamma^\mu \gamma_5 (\not{p}_1 + m_e) \gamma^\nu \gamma_5] \text{Tr}[(\not{k}_1 + m_\chi) \gamma_\mu \gamma_5 (\not{k}_2 - m_\chi) \gamma_\nu \gamma_5] \\ &= \frac{4}{\Lambda^4} [p_2^\mu p_1^\nu - g^{\mu\nu} (p_1 \cdot p_2) + p_2^\nu p_1^\mu + g^{\mu\nu} m_e^2] [k_{1\mu} k_{2\nu} - g_{\mu\nu} (k_1 \cdot k_2) + k_{1\nu} k_{2\mu} + g_{\mu\nu} m_\chi^2] \\ &= \frac{8}{\Lambda^4} [(p_2 \cdot k_1)(p_1 \cdot k_2) + (p_2 \cdot k_2)(p_1 \cdot k_1) - m_\chi^2 (p_1 \cdot p_2) - m_e^2 (k_1 \cdot k_2) + 2m_e^2 m_\chi^2] \\ &= \frac{8}{\Lambda^4} \left[ \frac{s^2}{16} (1 + \beta_e \beta_\chi \cos \theta)^2 + \frac{s^2}{16} (1 - \beta_e \beta_\chi \cos \theta)^2 - m_\chi^2 \left( \frac{s}{2} - m_e^2 \right) - m_e^2 \left( \frac{s}{2} - m_\chi^2 \right) + 2m_e^2 m_\chi^2 \right] \\ &= \frac{1}{\Lambda^4} [s^2 (1 + \beta_e^2 \beta_\chi^2 \cos^2 \theta) - 4s(m_\chi^2 \beta_e^2 + m_e^2 \beta_\chi^2)]. \end{aligned} \quad (86)$$

总截面为

$$\begin{aligned} \sigma &= \frac{\beta_\chi}{64\pi^2 s \beta_e} \int d\Omega \frac{1}{\Lambda^4} [s^2 (1 + \beta_e^2 \beta_\chi^2 \cos^2 \theta) - 4s(m_\chi^2 \beta_e^2 + m_e^2 \beta_\chi^2)] \\ &= \frac{s \beta_\chi}{16\pi \Lambda^4 \beta_e} \left[ 1 + \frac{1}{3} \beta_e^2 \beta_\chi^2 - \frac{4}{s} (m_\chi^2 \beta_e^2 + m_e^2 \beta_\chi^2) \right]. \end{aligned} \quad (87)$$

解析计算与 MadGraph 5 计算结果比较如下。

$$s = 250 \text{ GeV}, \quad m_\chi = 100 \text{ GeV}, \quad \Lambda = 1 \text{ TeV}, \quad \sigma = 0.139436 \text{ fb}, \quad \sigma_{\text{MG5}} = 0.13946 \text{ fb}. \quad (88)$$

对于算符  $\mathcal{O}_{\text{FA}}$ , 暗物质湮灭过程  $\chi\bar{\chi} \rightarrow ZZ$  是螺旋度压低的。

## B 算符 $\mathcal{O}_{\text{F1}}$ 和 $\mathcal{O}_{\text{F2}}$ 参数对产生截面的影响

若将算符  $\mathcal{O}_{\text{F1}}$  和  $\mathcal{O}_{\text{F2}}$  重新参数化为

$$\mathcal{O}_{\text{F1}} = \frac{1}{\Lambda^3} \bar{\chi} \chi (k_1 B_{\mu\nu} B^{\mu\nu} + k_2 W_{\mu\nu}^a W^{a\mu\nu}), \quad \mathcal{O}_{\text{F2}} = \frac{1}{\Lambda^3} \bar{\chi} i \gamma_5 \chi (k_1 B_{\mu\nu} \tilde{B}^{\mu\nu} + k_2 W_{\mu\nu}^a \tilde{W}^{a\mu\nu}), \quad (89)$$

则产生截面在  $k_1$ - $k_2$  平面上的大小变化如 Fig. 15 所示。

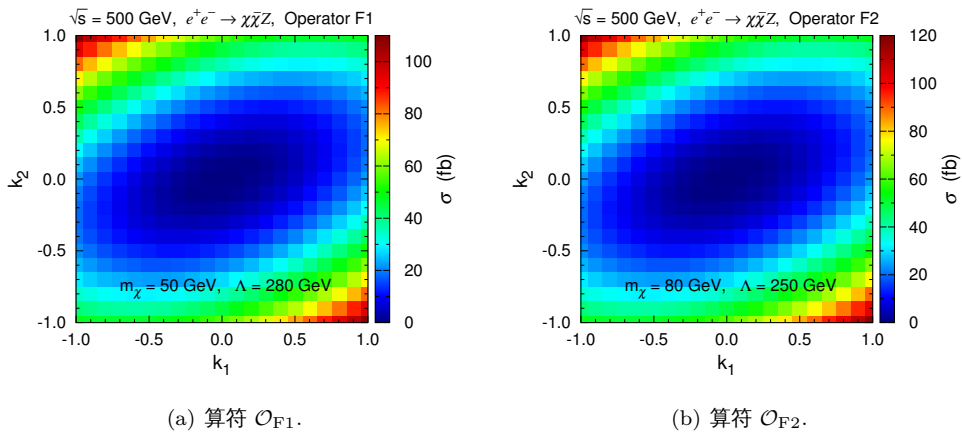


Figure 15: 产生截面在  $k_1$ - $k_2$  平面上的大小变化。

## C 背景和信号的极化截面

$\sqrt{s} = 500$  GeV 时, 主要背景和信号的极化截面如 Figs. 16 和 17 所示.

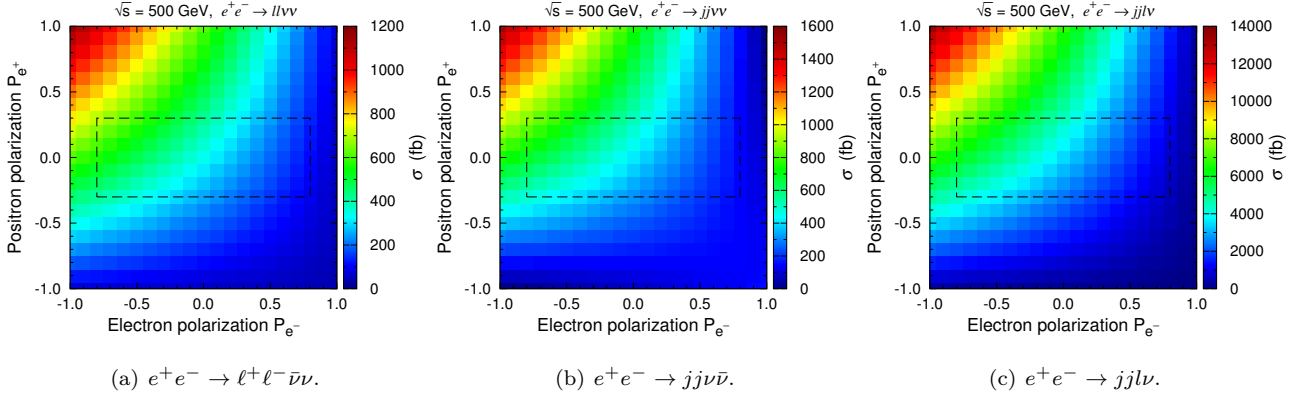


Figure 16: 主要背景的极化截面. 虚线方框表示极化度满足  $-0.8 \leq P_{e-} \leq +0.8$ ,  $-0.3 \leq P_{e+} \leq +0.3$  的区域.

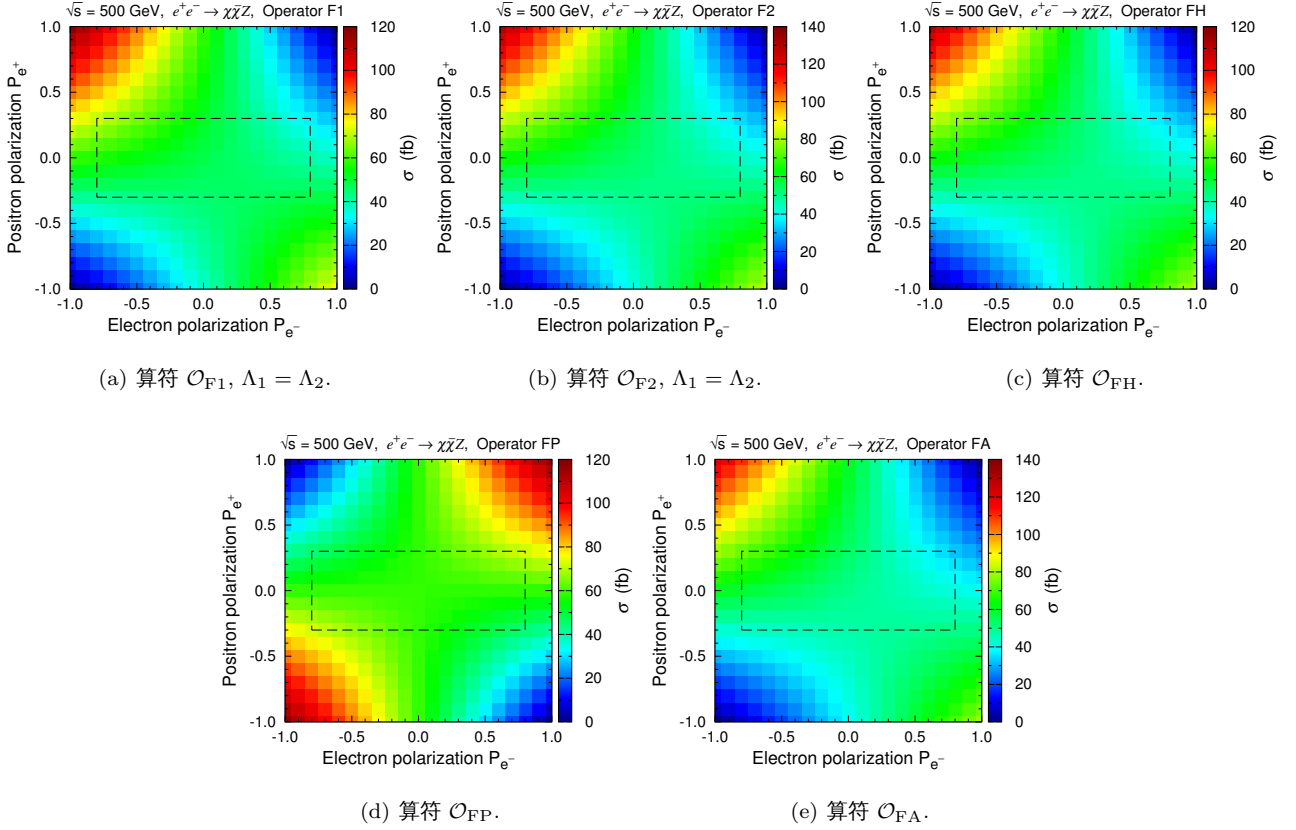


Figure 17: 信号的极化截面. 所取参数如 benchmark point (17) 所示. 虚线方框表示极化度满足  $-0.8 \leq P_{e-} \leq +0.8$ ,  $-0.3 \leq P_{e+} \leq +0.3$  的区域.

## D 末态角分布与螺旋度的关系: 一个例子

为了了解末态粒子角分布与螺旋度的关系, 这里对只含  $t$ -channel Feynman 图的  $e^-\bar{\nu}_e \rightarrow \gamma W^-$  过程进行分析, Feynman 图如 Fig. 18 所示. 在  $\sqrt{s} = 100$  GeV 的质心系中, 末态粒子螺旋度分布与角分布如 Fig. 19 所示. 当  $W$

玻色子螺旋度为正或零时, 光子动量倾向于与将它辐射出来的初态电子同向, 这是  $t$ -channel Feynman 图的性质. 由于只有左手电子才能发生  $e^-\bar{\nu}_e \rightarrow \gamma W^-$  过程, 在这样的事例中, 光子的螺旋度大多为负. 当  $W$  玻色子螺旋度为负时, 光子动量方向倾向于与束流方向垂直, 且其螺旋度没有倾向, 但这样的事例非常少.

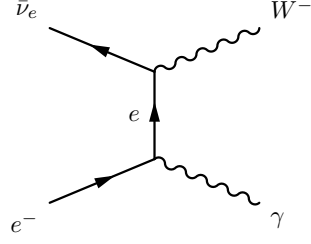


Figure 18:  $e^-\bar{\nu}_e \rightarrow \gamma W^-$  过程的  $t$ -channel Feynman 图.

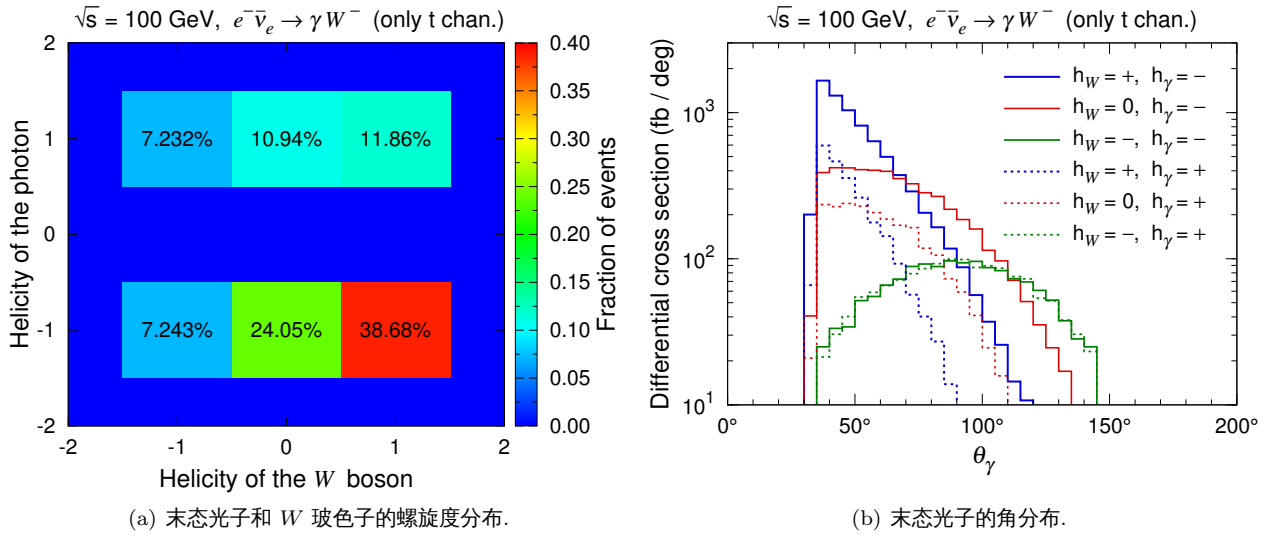


Figure 19: 只含  $t$ -channel Feynman 图的  $e^-\bar{\nu}_e \rightarrow \gamma W^-$  过程在质心系中的末态粒子螺旋度分布与角分布. 生成事例时要求末态光子满足  $p_T > 10$  GeV,  $|\eta| < 2.5$ , 质心系能量为 100 GeV.

## E 赝快度 $\eta$ 与 $\theta$ 角的对应关系

赝快度  $\eta$  与  $\theta$  角的关系为

$$\eta = -\ln \tan \frac{\theta}{2}, \quad \theta = 2 \tan^{-1}(e^{-\eta}). \quad (90)$$

由于  $\tan \frac{\pi - \theta}{2} = \cot \frac{\theta}{2}$ ,  $\ln \tan \frac{\theta}{2} + \ln \tan \frac{\pi - \theta}{2} = \ln \left( \tan \frac{\theta}{2} \cot \frac{\theta}{2} \right) = 0$ , 故

$$-\eta = \ln \tan \frac{\theta}{2} = -\ln \tan \frac{\pi - \theta}{2}. \quad (91)$$

可见,  $-\eta$  对应着  $\pi - \theta$ .

$\eta$  与  $\theta$  之间的数值如 Table 7 所示.

## 参考文献

- [1] N. F. Bell, J. B. Dent, A. J. Galea, T. D. Jacques, L. M. Krauss and T. J. Weiler, “Searching for Dark Matter at the LHC with a Mono-Z,” Phys. Rev. D **86**, 096011 (2012) [arXiv:1209.0231 [hep-ph]].

Table 7:  $\eta$  与  $\theta$  的对应关系.

$\eta$	0	0.5	1	1.5	2	2.5	3	4	5	10
$\theta$	90°	62.476°	40.395°	25.157°	15.415°	9.385°	5.700°	2.098°	0.772°	0.005°
$\eta$	4.74	3.64	3.13	2.44	2.03	1.74	1.32	1.01	0.76	0.36
$\theta$	1°	3°	5°	10°	15°	20°	30°	40°	50°	70°

- [2] L. M. Carpenter, A. Nelson, C. Shimmin, T. M. P. Tait and D. Whiteson, “Collider searches for dark matter in events with a Z boson and missing energy,” arXiv:1212.3352.
- [3] A. Alloul, N. D. Christensen, C. Degrande, C. Duhr and B. Fuks, “FeynRules 2.0 - A complete toolbox for tree-level phenomenology,” arXiv:1310.1921 [hep-ph].
- [4] J. Alwall, M. Herquet, F. Maltoni, O. Mattelaer and T. Stelzer, “MadGraph 5 : Going Beyond,” JHEP **1106**, 128 (2011) [arXiv:1106.0522 [hep-ph]].
- [5] T. Sjostrand, S. Mrenna and P. Z. Skands, “PYTHIA 6.4 Physics and Manual,” JHEP **0605**, 026 (2006) [hep-ph/0603175].
- [6] PGS-4, J. Conway et al., <http://www.physics.ucdavis.edu/~conway/research/software/pgs/pgs4-general.htm>.
- [7] T. Behnke, J. E. Brau, P. N. Burrows, J. Fuster, M. Peskin, M. Stanitzki, Y. Sugimoto and S. Yamada *et al.*, “The International Linear Collider Technical Design Report - Volume 4: Detectors,” arXiv:1306.6329 [physics.ins-det].
- [8] M. Ackermann *et al.* [Fermi-LAT Collaboration], arXiv:1310.0828 [astro-ph.HE].
- [9] T. Behnke, J. E. Brau, B. Foster, J. Fuster, M. Harrison, J. M. Paterson, M. Peskin and M. Stanitzki *et al.*, arXiv:1306.6327 [physics.acc-ph].